Adsorptive recovery of phosphate using biomass derived carbonaceous material and its feasibility in fertilizer use

By

Iqra Irfan

Registration No. 00000364934

Supervisor

Dr. Muhammad Ali Inam

A thesis submitted in partial fulfillment of the requirements for the degree of Master of Science in Environmental Engineering

Institute of Environmental Sciences and Engineering,

School of Civil and Environmental Engineering,

National University of Sciences and Technology

Islamabad, Pakistan

(2023)

APPROVAL CERTIFICATE

Certified that the contents and forms of the thesis entitled.

"Adsorptive recovery of phosphate using biomass derived carbonaceous material and its feasibility in fertilizer use "

Submitted by

Ms.

Iqra Irfan

Has been found satisfactory for partial fulfillment of the requirements of the degree of Master of Science in Environmental Engineering.

Supervisor: _____

Dr. Muhammad Ali Inam

Assistant Professor

SCEE (IESE), NUST

GEC Member: _____

Dr. Rashid Iftikhar

Assistant Professor

SCEE (IESE), NUST

GEC Member: _____

Dr. Zaib Jahan

Assistant Professor

SCME (CHEM), NUST

GEC Member: _____

Dr. Muhammad Hasaan

Associate Professor

USPCASE (ESE), NUST

ACCEPTANCE CERTIFICATE

It is certified that the contents and forms of the thesis entitled **"Adsorptive recovery of phosphate using biomass derived carbonaceous material and its feasibility in fertilizer use"** submitted by Ms. Iqra Irfan, Registration No. 00000364934 found complete in all respects as per NUST Regulations, is free of plagiarism, and mistakes and is accepted as partial fulfilments for award of MS degree. It is further certified that necessary modifications as pointed out by GEC members of the scholar have been included in the said thesis.

Supervisor: _____

Dr. Muhammad Ali Inam

SCEE (IESE), NUST

Head of Department: _____

Dated: 12/10/2023

Associate Dean: _____

Dated: 13 10-2023

Principal & Dean SCEE: _____

16 OCT 2023

Dated: _____

1

DECLARATION

I certify that this research work titled **"Adsorptive recovery of phosphate using biomass derived carbonaceous material and its feasibility in fertilizer use"** is my own work. This work has not been presented elsewhere for evaluation. The material that has been used from other sources has been properly acknowledged.

Iqra Irfan

00000364934

PLAGIARISM CERTIFICATE

I certify that this research work titled "Adsorptive recovery of phosphate using biomass derived carbonaceous material and its feasibility in fertilizer use" is my own work. Thesis has significant new work as compared to already published or under consideration to be published elsewhere. The thesis has been checked using TURNITIN and found within limits as per HEC plagiarism Policy and instructions issued from time to time.

Signature of Student:_____

Dr. Muhammad Ali Inam
Assistant Professor
IESE (SCEE) NUST Islamabad

Signature of Supervisor:_____

DEDICATION

This endeavor would not have been possible without the support of my exceptional parents, adored siblings, and my friends whose tremendous support and cooperation led me to this wonderful accomplishment.

"By virtue of whose prayers, we have been able to attain this position and whose hands are always raised for prayers, for our well-being."

ACKNOWLEDGEMENT

Contents

List of Figures

List of Tables

LIST OF ABBREVIATIONS

PO_4^{3-}	Phosphate ions
RBC	Raw Biochar
WBC	Whet Straw Biochar
SBC	Sewage Sludge Biochar
CBC	Combined Biochar
Fe@WBC	Iron Modified Wheat Straw Biochar
Fe@SBC	Iron Modified Sewage Sludge Biochar
Fe@CBC	Iron Modified Combined Sewage Sludge
AR:Fe@WBC	Phosphate Sorbed Iron Modified Wheat Straw Biochar
AR:Fe@SBC	Phosphate Sorbed Iron Modified Sewage Biochar
AR:Fe@CBC	Phosphate Sorbed Iron Modified Combined Biochar

ABSTRACT

In recent years, the removal and recovery of phosphate (PO_4^{3-}) from freshwater reservoirs using carbonaceous adsorbents has received much attention to address eutrophication issues and plant phosphate requirements. The viability of $FeCl_3$ impregnated biochar (Fe@CBC) synthesized via co-pyrolysis of wheat straw (WS) and sewage sludge (SS) for phosphate removal from water under systematically designed sorption experiments and its subsequent potential as phosphatic fertilizer for improving plant growth, was thoroughly investigated in this study. The relatively higher PO_4^{3-} sorption performance of Fe@CBC (5.23 mg/g) compared to $FeCl_3$ impregnated biochars (Fe@WBC: 4.16 mg/g and Fe@SBC: 5.14 mg/g) synthesized via separate pyrolysis of WS and SS were primarily ascribed to the nano porous structure, higher point of zero charge (pH_{pzc}) and enriched iron complexes on its surface (Fe-OH and FeC). Consequently, dominant sorption mechanism of PO_4^{3-} ions towards Fe@WBC was associated to ligand exchange and chemisorption whereas that of Fe@SBC and Fe@CBC was identified as electrostatic surface complexation coupled with reduction. In comparison to Fe@WBC and Fe@SBC, the surface properties and identified phenomenon allowed Fe@CBC to efficiently recover PO_4^{3-} ions under optimal water chemistry conditions and coexisting interfering species environment. Additionally, PO_4^{3-} -sorbed Fe@CBC effectively improved the physical growth (root length: 2 cm, shoot length: 9 cm, fresh weight: 79 mg and dry weight: 8.3 mg) of mustard plants. Economic analysis suggested profit of PO_4^{3-} removal and recovery by Fe@CBC was $1.5 per Kg. Therefore, PO_4^{3-} -sorbed Fe@CBC could be a promising phosphatic fertilizer for improving plant growth and may have agricultural applications.

<div align="right">

Chapter 1

</div>

INTRODUCTION

1.1 Background

1.1.1 Introduction to Phosphorus

Phosphorus, an essential element for sustaining life, plays a crucial role in maintaining global food production and ensuring food security. Its significance stems from its involvement in nucleic acids, cell membranes, and adenosine triphosphate (ATP), the energy currency of cells. As the world's population continues to grow, the demand for phosphate-based fertilizers increases, putting strain on limited phosphate rock reserves (Gilbert, 2009). This heightened demand also exacerbates the environmental impacts associated with conventional phosphate mining and fertilizer production.

1.1.2 Sources

Phosphate, a critical and irreplaceable nutrient, is abundant in the environment and comes from a variety of sources, including natural geological processes, human activities, and biological interactions. Understanding the complexities of phosphorus dispersion in our ecosystems requires a thorough understanding of these various sources. Here are some of the key sources of phosphate (PO_4^{3-}) in the environment, each of which plays a specific function in the complex phosphorus cycle:

1.1.2.1 Natural Geological Deposits

Phosphate-rich geological formations, such as sedimentary rocks containing PO_4^{3-} minerals such as apatite, serve as the Earth's natural reservoirs for this critical nutrient. These deposits form the basis for PO_4^{3-} extraction and usage.

1.1.2.2 Agricultural Runoff

Phosphate-based fertilizers are frequently used in modern agriculture to increase crop yields. When rain or irrigation water interacts with crops treated with these fertilizers, excess PO_4^{3-} might wash off, contributing to agricultural runoff. This runoff transports excess PO_4^{3-} into neighbouring bodies of water, resulting in water contamination and eutrophication.

1.1.2.3 Sewage and Wastewater

Human activities generate significant volumes of wastewater, including sewage from residences and industrial effluent from many sectors. These wastewater streams frequently contain PO_4^{3-} compounds from detergents and human waste. Inadequate wastewater treatment or incorrect disposal of wastewater can result in the discharge of PO_4^{3-} into aquatic habitats.

1.1.2.4 Natural Weathering

PO_4^{3-} is found naturally in rocks, minerals, and organic substances. Weathering processes degrade these substrates over geological timeframes, eventually releasing PO_4^{3-} ions into soil and water. This natural release is critical to nutrient cycling throughout ecosystems.

1.1.2.5 Wildlife and Organic Matter

Organic compounds, such as animal manure and decomposing plant matter, can act as PO_4^{3-} reservoirs. Furthermore, wildlife behaviours such as nesting and foraging help to redistribute phosphorus within ecosystems. These organic sources are critical in nutritional dynamics.

1.1.2.6 Aquatic Sediments

PO_4^{3-} builds up in the sediments at the bottoms of bodies of water over time. PO_4^{3-} can be discharged from sediments into the water column under certain conditions, such as low oxygen levels. This phenomenon has an impact on water quality and nutrient cycling in aquatic habitats.

1.1.2.7 Industrial Discharges

Phosphate-containing wastewater is generated by a variety of industrial operations. Food processing, chemical manufacture, and mining all emit phosphate-rich effluents into the environment, which may have an impact on neighbouring ecosystems and water bodies.

1.1.2.8 Atmospheric Deposition

PO_4^{3-} can enter the environment through atmospheric deposition, which occurs when fine PO_4^{3-} particles are carried by the wind across vast distances. These particles eventually settle on land or sea surfaces, increasing PO_4^{3-} levels in a variety of habitats.

1.1.2.9   Fossil Fuel Combustion

The combustion of fossil fuels, such as coal and oil, emits PO_4^{3-} compounds into the environment as air pollutants. These chemicals can eventually settle on land and water surfaces, harming soil, and water quality.

1.1.2.10   Natural Sources

PO_4^{3-} compounds can be released into the environment by natural processes such as volcanic eruptions and geothermal activity. Furthermore, PO_4^{3-} can be found naturally in a variety of minerals and mineralized streams.

These numerous sources alter PO_4^{3-} availability and distribution in ecosystems, influencing nutrient cycle, plant development, and water quality. Proper management and understanding of these sources are vital for striking a balance between the critical role of PO_4^{3-} in life support and the potential environmental risks associated with its accumulation.

1.1.3   Traditional Methods of Phosphate extraction

Traditional methods of PO_4^{3-} extraction heavily rely on mining finite PO_4^{3-} rock deposits, leading to habitat disruption, land degradation, and various environmental concerns. Furthermore, the subsequent processing and distribution of phosphate-based fertilizers contribute to greenhouse gas emissions and foster nutrient imbalances in ecosystems, resulting in water pollution, particularly through agricultural runoff.

1.2 Environmental Significance

The research conducted in this study holds significant importance within the environmental field due to the urgent requirement to address the ecological repercussions associated with the use of phosphates in agriculture. Furthermore, the study aims to establish a sustainable phosphorus supply for future generations. The investigation focuses on several crucial aspects of environmental significance:

1.2.1   Water Pollution Mitigation

Water pollution mitigation is a critical concern at present, with particular attention directed towards the issue of phosphate runoff originating from agricultural fields. This runoff, characterized by high levels of soluble phosphate, infiltrates freshwater bodies and coastal zones, ultimately leading to the occurrence of eutrophication. Eutrophication, in turn, has the potential to significantly disrupt aquatic ecosystems, negatively impact biodiversity, and pose substantial threats to human health. Given the wide-ranging impacts of PO_4^{3-} runoff and

eutrophication, it is crucial to develop effective strategies for water pollution mitigation. Implementing sustainable agricultural practices, such as precision nutrient management and the use of cover crops, can help reduce the excessive use of phosphorus-based fertilizers and consequent runoff. Additionally, the implementation of buffer zones and wetlands can serve as natural filters, capturing and retaining excess nutrients before they reach water bodies.

1.2.2 Resource Conservation

PO_4^{3-} rock reserves are limited and concentrated in a few places throughout the world. As these deposits' finite, ensuring a consistent PO_4^{3-} supply for future generations becomes increasingly difficult. Our findings highlight the importance of using biomass-derived carbonaceous materials for PO_4^{3-} recovery, providing a sustainable, circular method that reduces dependency on PO_4^{3-} mining and encourages the prudent use of existing resources.

1.2.3 Climate Change Mitigation

Traditional PO_4^{3-} mining and fertilizer manufacturing methods are energy-intensive and contribute to greenhouse gas emissions, often resulting in resource inefficiency and waste. In contrast, our alternative approach, based on PO_4^{3-} recovery from renewable biomass sources, not only has the potential to significantly reduce the carbon footprint associated with phosphate-based fertilizer production, but it also improves resource efficiency by repurposing underutilized materials. This shift to a more effective and sustainable resource use paradigm encourages localized and decentralized production, decreasing the need for substantial raw material transportation and promoting regional economic development. Furthermore, it supports the concept of a circular phosphorus economy, in which phosphorus is continuously recycled and reused, reducing dependency on new PO_4^{3-} rock extraction, and resolving environmental concerns.

1.2.4 Support for Sustainnable Agriculture

Conventional PO_4^{3-} mining and fertilizer production techniques utilize a lot of energy and contribute to greenhouse gas emissions. Our alternative technique, based on PO_4^{3-} recovery from renewable biomass sources, has the potential to significantly reduce the carbon footprint associated with phosphate-based fertilizer manufacturing. This is in line with global efforts to tackle climate change by shifting to more sustainable and energy-efficient methods. This work, which focuses on PO_4^{3-} recovery from renewable biomass sources, offers considerable reductions in the carbon footprint associated with the manufacturing of phosphate-based fertilizer. It fits in perfectly with global climate action and sustainable practices.

In view of these serious environmental issues and prospects, this thesis launches a thorough and complex inquiry into the adsorptive recovery of PO_4^{3-} utilizing carbonaceous materials obtained from biomass. Our research aims not only to increase scientific understanding of this novel technique, but also to contribute effectively to long-term solutions that address the immediate and long-term environmental challenges related with PO_4^{3-} usage in agriculture.

1.3 Problem Statement

The use of functionalized biochar as an adsorbent material represents a prospective path for PO_4^{3-} adsorption in a variety of applications, including water treatment, environmental protection, and agricultural sustainability. The pressing issue at hand is the creation of stable adsorbents that not only remove PO_4^{3-} efficiently but also allow for an equally efficient recovery and regeneration process, assuring their long-term sustainability. This need for stability and sustainability is especially important in the field of water management, where PO_4^{3-} level regulation is critical in maintaining water quality, protecting aquatic habitats, and combating the negative effects of eutrophication.

Eutrophication, which is mostly caused by high PO_4^{3-} levels in bodies of water, poses a serious threat to the natural balance of freshwater ecosystems. It disturbs aquatic life's natural rhythms, destroys biodiversity, and has a negative impact on the health of both aquatic organisms and humans who rely on these ecosystems. As a result, the development and application of effective and stable PO_4^{3-} adsorption techniques, such as those based on functionalized biochar, has become critical in mitigating these ecological difficulties and assuring the preservation of our crucial water resources.

1.4 Objectives

This study goes on a complex examination at the intersection of materials engineering, environmental chemistry, and agricultural innovation, in an era marked by environmental consciousness and the requirement of sustainable practices. In the face of mounting environmental challenges, efficient management of phosphorus, a life-sustaining element and critical component of global food production, has emerged as a top priority. Traditional PO_4^{3-} mining and fertilizer manufacture processes, while necessary for agricultural productivity, have not been without consequences, including water contamination and resource depletion. In response to these critical concerns, the research objectives of this study are reflected as follows:

i)   Synthesize and compare the surface properties of Fe functionalized BC obtained from SS, WS, and their mixed proportions.

ii)   To examine the influence of water chemistry parameters on the sorption behaviour of modified BC towards PO_4^{3-} ons

iii) The technoeconomic evaluation of modified BC for PO_4^{3-} recovery and its utilization as an alternative fertilizer for mustard plant growth.

<div align="right">**Chapter 2**</div>

LITERATURE REVIEW

PO_4^{3-} is a non-renewable, yet necessary nutrient derived from naturally occurring phosphorous rocks that can enter water reservoirs via urban and agricultural operations. This dual role of PO_4^{3-} as both vital and finite emphasizes the critical requirement for long-term PO_4^{3-} management. (Gilbert, 2009). Excess PO_4^{3-} in lake environments can cause eutrophication, resulting in destructive algal blooms and posing serious hazards to the ecology. This dual effect emphasizes the critical importance of proper PO_4^{3-} control and management in aquatic systems. (Li et al., 2023; Suazo-Hernández et al., 2023). Recognizing the critical relevance of water quality in the preservation of the natural environment, the World Health Organization (WHO) set a maximum allowable limit for total phosphate at 0.1 mg/L. This shows the global commitment to protecting freshwater ecosystems and human health from the harmful consequences of PO_4^{3-} contamination (Owens & Shipitalo, 2006) (WHO, 2017). Meeting drinking water quality standards and managing PO_4^{3-} shortages necessitate the employment of innovative technologies that secure the long-term usage of this crucial resource while also protecting our environment. These novel approaches are critical in establishing a balance between human needs and environmental protection.

2.1 Phosphate removal technologies

Previous research has thoroughly investigated numerous treatment systems for PO_4^{3-} removal from water. These studies sought to address the issues raised by high PO_4^{3-} levels in natural water bodies, which can cause eutrophication, hazardous algal blooms, and negative ecological effects. Several therapy strategies have been studied and developed, each with its own set of benefits and drawbacks. such as membrane (nano) filtration, electrochemical procedures, chemical precipitation, and ion exchange to remove PO_4^{3-} from water source.

2.1.1 Membrane Filtration

PO_4^{3-} ions have been removed from water using membrane filtering techniques such as nanofiltration and reverse osmosis (Beaudry & Sengupta, 2021).These technologies extract PO_4^{3-} molecules from water using semipermeable membranes, resulting in purified water with lower PO_4^{3-} contents. These technologies, however, can be energy-intensive and expensive to adopt on a broad scale.

2.1.2 Electrochemical Methods

Electrochemical methods for PO_4^{3-} removal offer an environmentally friendly and efficient approach (Leo et al., 2011). By using electrodes to induce redox reactions, PO_4^{3-} ions are electrochemically transformed into solid compounds, minimizing the need for chemicals, and generating less sludge. This innovative technology is gaining recognition for its potential in sustainable water treatment solutions.

2.1.3 Chemical Precipitation

Chemical precipitation is a popular method for eliminating PO_4^{3-} from water, which aids in the fight against water pollution and eutrophication (Owodunni et al., 2023). It facilitates the production of PO_4^{3-} flocs, which may be easily separated from the treated water, by adding coagulants and optimizing pH. However, efficient sludge management is critical to ensuring the process's environmental sustainability.

2.1.4 Ion Exchange

Ion exchange resins can absorb PO_4^{3-} ions from water selectively by exchanging them with other ions on the resin surface (Y. Ren et al., 2022). The resin can be regenerated for reuse after being soaked with PO_4^{3-}. Although ion exchange is effective, it may necessitate periodic resin replacement and chemical regeneration.

While these technologies provide feasible PO_4^{3-} removal methods, they are not without downsides. Many of them are energy-intensive, produce a lot of sludge, and require constant maintenance. Efforts to reduce PO_4^{3-} pollution and its negative effects on water quality and ecosystems necessitate a thorough assessment that considers not only the effectiveness of various treatment technologies but also their economic feasibility, energy efficiency, and environmental consequences. A comprehensive approach that integrates these elements is thought critical for identifying sustainable and practical PO_4^{3-} removal methods in a variety of situations.

2.2 Phosphate removal by adsorption

Adsorption has evolved as a highly successful approach for eliminating PO_4^{3-} anions from water sources as an environmentally acceptable and efficient treatment technology. This method is based on the ability of certain materials, known as adsorbents, to attract and bind PO_4^{3-} ions from water onto their surfaces. The following is an explanation of how PO_4^{3-} removal by adsorption works:

2.2.1 Choice of Adsorbent

For PO_4^{3-} removal, several adsorbent materials such as activated carbon, metal oxides, clay minerals, and biomass-derived compounds such as biochar can be utilized. Adsorbent selection is influenced by factors such as cost, availability, and PO_4^{3-} adsorption efficacy.

2.2.2 Adsorption Mechanism:

Adsorption removes PO_4^{3-} effectively by attracting PO_4^{3-} ions to the adsorbent's surface via electrostatic interactions and chemical bonding. Recent work, such as that of Z. Ajmal et al. (B. Liu et al., 2022) has focused on mechanisms such as ligand exchange and inner sphere complexation, particularly in metal-based adsorbents.

2.2.3 Surface Modification:

Adsorbents can be changed in some circumstances to improve their PO_4^{3-} adsorption capacity. Surface changes can include functionalization with certain chemicals or metals to boost binding affinity of PO_4^{3-} ions.

2.2.4 Batch or Column Studies:

PO_4^{3-} removal research can be carried out in batch experiments or in continuous flow column tests. In batch trials, a known amount of adsorbent is mixed with a phosphate-containing solution for a predetermined amount of time. In column research, water is constantly run through a packed bed of adsorbent to remove phosphate.

2.2.5 Adsorption Isotherms:

Adsorption isotherms are used to describe the relationship between the concentration of PO_4^{3-} in water and the amount of PO_4^{3-} absorbed by the adsorbent. Common models, such as the Langmuir and Freundlich isotherms, assist characterize adsorption behaviour.

2.2.6 Kinetics:

Adsorption kinetics show how quickly PO_4^{3-} ions are adsorbed onto the surface of an adsorbent. Adsorption rates are analysed using common kinetic models such as the pseudo-first-order and pseudo-second-order models.

2.2.7 Regeneration:

Phosphate-loaded materials can typically be regenerated to recover PO_4^{3-} or correctly dispose of it, depending on the adsorbent. Washing the adsorbent with a solution that desorbs PO_4^{3-} ions may be used in regeneration, allowing for reuse or safe disposal of the concentrated phosphate.

2.2.8   Practical Applications:

Adsorption of phosphorus has practical applications in wastewater treatment, water purification, and agricultural nutrient control. It can be used to lower PO_4^{3-} levels in industrial effluents, municipal sewage, and eutrophicated natural water bodies.

2.2.9   Environmental Considerations:

PO_4^{3-} removal by adsorption is a cost-effective and versatile technique for reducing PO_4^{3-} pollution, contributing to better water quality and healthier ecosystems in a variety of industries. However, the environmental impact of discarded adsorbents and the handling of concentrated PO_4^{3-} must be considered.

While these approaches considerably improve PO_4^{3-} removal efficiency, there is serious worry about metal leakage from these sorbents into aquatic systems, which can worsen toxicological implications. As a result, the development of long-lasting and highly efficient sorbents is critical in tackling PO_4^{3-} contamination in drinking water. These improved sorbents must strike a difficult balance between enhancing PO_4^{3-} removal capabilities and limiting potential environmental consequences. This novel approach to adsorption technology is critical in our pursuit of cleaner, safer drinking water, ensuring that solutions do not generate new issues along the way.

2.3 Biochar for Phosphate adsorption

Sustainable techniques, such as using biomass-derived adsorbents like biochar, provide a more environmentally friendly option. A wide range of researchers (Z. Liu & Balasubramanian, 2013; Sakhiya et al., 2020) have explored the potential of agro-biomass residues and sewage sludge (SS) for production of biochar (BC). Pakistan is 8th largest producer of wheat grains however around 40.5 million tons of wheat straw residues is openly burnt, thus affecting the overall climate (Bheel et al., 2021). Moreover, due to the rapid urbanization in the country, the production of SS has also substantially increased (Riaz et al., 2020). The increased amount of SS generation rises serious concerns about its safe disposal because of its hazardous composition (Li et al., 2023). Various thermal and physicochemical techniques have been employed to treat SS. Amongst, pyrolysis is considered as promising technology for the eventual disposal of sludge as it has the potential to significantly reduce its volume, eliminate pathogens and parasites, and completely decompose the organic residues. Additionally, both SS and agro biomass i.e., wheat straw (WS) can be transformed into value added product (BC) through pyrolysis. However, raw BC presents insignificant phosphate

removal and reclamation potential because of electrostatic hindrance (X. Q. Liu et al., 2016). Therefore, surface modification including metal-based impregnation of the BC may improve PO_4^{3-} adsorption from aquatic media.

Biochar (BC) formed from biomass has received a lot of interest in recent years as a versatile and sustainable substance for removing PO_4^{3-} from water sources. Various varieties of BC have been investigated for their PO_4^{3-} adsorption capacities, and they have been proven as a viable remedy to PO_4^{3-} pollution.

Notably, the PO_4^{3-} adsorption capacity of BC produced from various sources such as dewatered dry sludge, rice husk, and wood waste (WS) has been examined. These BC materials have been modified, with the addition of iron (Fe), chitosan, lanthanum, calcium, and other functional groups to improve their adsorption capabilities. This wide range of BC feedstocks and alterations demonstrates the adaptability of BC-based adsorbents to various water quality scenarios and environmental conditions (Ajmal et al., 2020; Feng et al., 2021; M. Liu et al., 2022; Ren et al., 2021; Shakoor et al., 2021; Yang et al., 2018).

Activated biochar, which have excellent PO_4^{3-} removal characteristics, have received a lot of attention in this field. Physical, chemical, or thermal activation techniques dramatically enhance the surface area and porosity of BC, providing more active sites for PO_4^{3-} binding. Because of their increased adsorption ability, activated biochar are a promising method for tackling PO_4^{3-} contamination issues.

Furthermore, the use of BC for PO_4^{3-} removal is consistent with sustainability standards. BC is frequently created from renewable biomass sources, providing an environmentally beneficial alternative to traditional treatment procedures. Its intrinsic stability and resistance to degradation make it a long-lasting adsorbent in PO_4^{3-} removal applications.

The importance of biomass-derived biochar as an efficient and environmentally responsible PO_4^{3-} adsorbent becomes clearer in the context of sustainable PO_4^{3-} management. Its adaptability, versatility, and eco-friendliness make it an appealing option for those seeking cleaner and better water resources. The current study investigates BC's potential, surface qualities, and ability to handle PO_4^{3-} pollution concerns, thereby contributing to the growing knowledge base in sustainable water treatment procedures.

Co-pyrolysis of SS with rice husk and eggshells have shown strong PO_4^{3-} sorption potential from water (Xiong et al., 2021). The co-pyrolysis of SS with lignin has also

presented synergistic removal performance of methylene blue from wastewater (Dai et al., 2022). Earlier research (Yang et al., 2018) also examined the effectiveness of Fe impregnated waste activated sludge BC for PO_4^{3-} removal from water. Among Fe-based compounds, $FeCl_3$ impregnated BC demonstrated strong PO_4^{3-} sorption affinity, as iron existed in hematite and amorphous hydroxide forms (Yang et al., 2018). However, literature seems scarce to study the sorption potential of sorbent synthesized from agricultural (WS) and non-agricultural (SS) waste to remove and recover PO_4^{3-} from water. In accordance, to the best of our knowledge, PO_4^{3-} removal and recovery by $FeCl_3$ modified BC synthesized via co-pyrolysis of WS and SS has not yet been studied.

MATERIALS AND METHODS

3.1 Materials and Reagents

Wheat straw (WS), an agricultural biomass, was gathered from a local field in District Attock, Punjab, Pakistan. Following that, WS was washed with distilled water, air dried, then oven dried overnight at 70^0 C. Furthermore, sewage sludge (SS) was collected from the MBR plant at the National University of Science and Technology in Islamabad, Pakistan, and oven dried for 24 hours at 100^0 C. The dried WS and SS samples were ground and sieved through a 0.2 mm screen to produce wheat straw powder (WSP) and sewage sludge powder (SSP), which were then sealed in airtight bags.

The reagent grade chemicals including potassium dihydrogen phosphate (KH_2PO_4), ferric chloride hexahydrate ($FeCl_3 \cdot 6H_2O$), ammonium molybdate tetrahydrate, ammonium metavanadate were obtained from Sigma Aldrich (USA). Other chemicals including sodium nitrate ($NaNO_3$), nitric acid (HNO_3), hydrochloric acid (HCl), sodium hydroxide (NaOH) magnesium chloride hexahydrate ($MgCl_2 \cdot 6H_2O$), potassium Nitrate (KNO_3), Potassium sulfate (K_2SO_4), Sodium bicarbonate ($NaHCO_3$) and Silicon dioxide (SiO_2) were obtained from local supplier. The 1000 mg/L PO_4^{3-} stock solution was prepared by dissolving KH_2PO_4 in distilled (DI) water obtained using distillation assembly. Moreover, working solution of desired PO_4^{3-} concentration was prepared by spiking required concentration of PO_4^{3-} in water as per experimental conditions.

3.2 Preparation of raw and iron modified biochar

Three different raw biochars (RBC) i.e., wheat straw biochar (WBC), sewage sludge biochar (SBC) and combined biochar (CBC) were obtained by pyrolysis of WS, SS and WS: SS (at equal ratio of 1:1) under nitrogen environment at 550°C for 3 hours (Niazi et al., 2018). Afterwards, all three RBC were sieved through 0.04 mm and stored in airtight bags.

3.2.1 Yield of pyrolysis

Results show in Table (1) show the yield of biochar, biogas, and bio-oil after pyrolysis of different biomasses including WSP, SSP and WSP: SSP (1:1), respectively. Among studied biomasses WSP presented lowest fraction of biochar yield (27.87 %) as compared to SSP (80.39 %) and WSP: SSP (55.20 %). Such observation may be attributable to the presence of higher fraction of hemicellulose and cellulose content in wheat straw, that may undergo

thermal decomposition to form greater quantity of bio-oil and biogas when compared with other biomasses (Venkatesh et al., 2022). Moreover, higher biochar yield observed in case of SSP and WSP: SSP may be ascribed to the presence of higher organic matter content in sewage sludge (Singh et al., 2020). The fraction of other pyrolysis products observed for WSP, SSP and WSP: SSP was (Bio-oil: 24.11 %, 6.46 % and 12.77 %) and (Biogas: 48.02 %, 13.15 % and 32.05 %), respectively.

Table 1 (%) Yield of pyrolysis

Materials	Yield (%)		
	Syn Gas	Bio Oil	Bio Char
Wheat straw powder	48.02	24.11	27.87
Sewage Sludge powder	13.15	80.39	80.39
Combined powder	32.05	12.77	55.2

3.2.2 Fe-modification of Biochar

Previously, it has been observed that the type of Fe-based salts as BC modifier pose a significant impact on contaminant removal from water (Yang et al., 2018). Therefore, we used ferric chloride hexahydrate ($FeCl_3 \cdot 6H_2O$) rather than other Fe-based salts, owing to its improved performance of BC towards PO_4^{3-} adsorption from water. For modification of RBC, 10g of raw RBC were mixed with (3g as Fe) $FeCl_3 \cdot 6H_2O$ in 500 distilled (DI) water and heated at 50°C to form a stable suspension (Nguyen et al., 2019). Afterwards, 0.05 M NaOH was added to suspension dropwise to raise pH to 11 and then allowed to mix for 1 hour. The organic residues were removed by washing modified BC with DI water until pH reaches 7. The BC composite was filtered using 0.22 μm GE cellulose nylon membrane filter, dried and stored in brown airtight desiccator. The Fe modified biochars (Fe@BC) obtained from raw WBC, SBC and CBC were finally represented as Fe@WBC, Fe@SBC, and Fe@CBC, respectively. The filtrate was also tested for residual Fe concentration using atomic absorption spectrophotometer (AAS, NovAA 800D, Analytik Jena, Germany).

3.3 Adsorption experiments

A series of batch experiments were conducted in 250 mL conical flasks to evaluate the removal potential of PO_4^{3-} from aqueous matrices. Initially, we investigated the influence of Fe@BC dosages (0.1, 0.2, 0.5, 1, 2, 3, 4, 5 g/L) using 100 mL PO_4^{3-} solution (10 mg/L, pH 7) with 2 hrs. stirring time. Kinetic studies were conducted by varying contact time (0, 15, 30, 60, 90, 120, 240, 480 min) using 100 mL PO_4^{3-} solution (10 mg/L, pH 7), and 0.2 g/L Fe@BC. Isotherm studies were conducted by varying initial PO_4^{3-} concentration (0, 1, 2, 3, 4,

5, 10, 15, 20, 25, 50 mg/L) at solution conditions (pH 7, contact time 3 hrs.), and 0.2 g/L Fe@BC. The influence of suspension pH (2, 5, 7, 9) using 100 mL PO_4^{3-} solution (10 mg/L, contact time 3 hrs.), and 0.2 g/L Fe@BC) was also examined. The follow up experiments were conducted using 100 mL PO_4^{3-} solution (pH 7, 10 mg/L, contact time 3 hrs.), and 0.2 g/L Fe@BC). Moreover, the influence of interfering species was also monitored under varying concentrations of 10, 50 and 100 mg/L of diverse anionic species (SO_4^{2-}, NO_3^-, Si^{2-}, HCO_3^-, Cl^- and mixed ions). Regeneration potential of Fe@BC were also monitored up to 5 cycles using 1M NaOH. The PO_4^{3-} concentration was analysed in the filtrate using UV-visible spectrophotometer (SPECORD 200 of Analytik Jena Germany) at 470 nm by molybdenum method (Y. Wang et al., 2019).

3.3.1 Kinetic Models

Kinetic models are used to describe and forecast the pace at which chemical reactions or processes, such as PO_4^{3-} adsorption by biochar, occur over time.

Details of kinetics models is as follows:

PSO equation:
$$qt = \frac{k2 * qe2 * t}{1 + k2qet}$$
(1)

PFO equation:
$$qt = qe - e^{\ln(qe) - K1(t)}$$
(2)

where t (min) was the contact time, q_e and qt were the adsorption quantity of PO_4^{3-} ions (g/mol) at the equilibrium condition and different time intervals, respectively; k_1 (1/min), k_2 (mol/g.min) were PFO, PSO rate constant respectively.

3.3.2 Isotherm Models

Isotherm models are used to understand and quantify the equilibrium relationship between a substance's concentration (such as PO_4^{3-} ions) adsorbed onto a surface (biochar) and its concentration in the surrounding solution. These models are useful for developing and optimizing adsorption processes.

Isotherm models used are as follows:

Langmuir Equation:
$q_e = (qm*k*C_e)/(1+k*C_e$
(3)

Freundlich Equation:
$q_e = k*(C_e^{(1/n)})$
(4)

where qe (g/mol) was the quantity of PO_4^{3-} ions sorbed onto Fe@BC surface, Ce (mg/L) was the quantity of PO_4^{3-} ions retained in the suspension; qm (g/ mol) was the maximum adsorption capacity, kL (L/mg) was Langmuir constant related to adsorption energy, kF

[(g/mol) (L/mg)]1/n was a constant related to the adsorption capacity, and n was an index of heterogeneity.

3.3.3 Thermodynamic Models

To examine the feasibility and effectiveness of PO_4^{3-} adsorption by biochar, thermodynamic models are used, assisting in the development of sustainable water treatment systems. Model used for thermodynamics is as follows:

Distribution coefficient: $\quad\quad\quad\quad kd = (Co - Ce\ Ce\ ) \times 1\ Cs$ **(5)**

Gibbs free energy: $\quad\quad\quad\quad\quad\quad \Delta G = -RTlnkd$ **(6)**

Thermodynamics parameters: $\quad\quad\quad \Delta G = \Delta H - T\Delta S$ **(7)**

where kd (mL/g) represent coefficient of distribution in PO_4^{3-} sorption, Cs (g/mL) was concentration formed in PO_4^{3-} ions, R was gas constant (8.314 J/mol.◦K), and T was temperature (◦K). ΔG and ΔH were standard changes in energy and enthalpy (KJ/mol) and ΔS (KJ/ mol.◦K) was the entropy of reaction. The linear fitting of ΔG versus T plot provides ΔH (intercept) and ΔS (slope) values.

3.3.4 Calibration Curve

Calibration curve of PO_4^{3-} solutions were prepared with R^2 value of 0.9962.
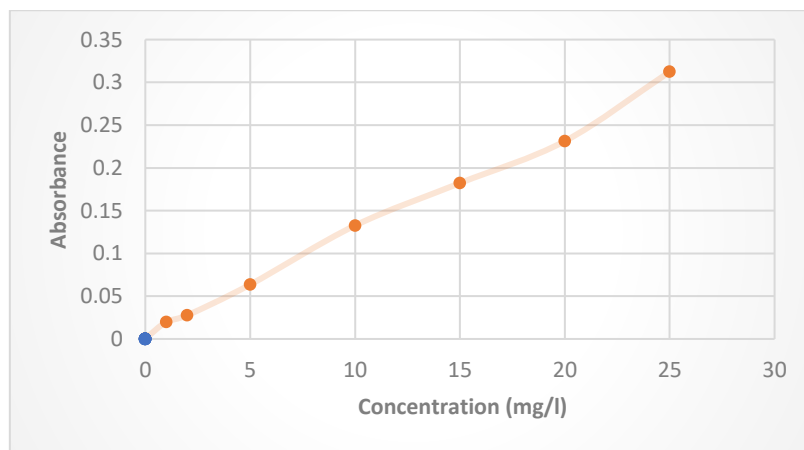
Figure 1 Calibration Curve

The removal efficiency (%) and adsorption capacity (mg/g) were calculated using **Eq (8)** and **Eq (9)** respectively:

$Removal\ efficiency : R\ (\%) = \frac{Co - Ce}{Co}\ 100$ $\quad\quad\quad\quad\quad\quad\quad\quad$ (8)

$Adsorption\ capacity : qe\ \left(\frac{mg}{g}\right) = \frac{(Co - Ce)}{Cs}$ $\quad\quad\quad\quad\quad\quad\quad\quad$ (9)

16

where C_o (mg/L) and C_e (mg/L) represent initial and residual PO_4^{3-} concentration, and C_s (g/L) indicate applied Fe@BC dosage under experimental conditions.

3.4 Analytical methods

3.4.1 Heavy metals and Phosphate content analysis

Raw powders, RBC and Fe@BC were digested according to standard procedures:

3.4.1.1 Digestion procedure for heavy metals analysis

To the sample, 9 mL of freshly prepared acid mixture of 65 % HNO_3 was added, and 37 % HCl (nitric-hydrochloric acid; 1:3) was added. Then, the mixture was boiled gently over a water bath (95 °C) for 4–5 h (or until the sample had completely dissolved).

3.4.1.2 Digestion procedure for phosphate content analysis

Condensed phosphorus is not readily available as reactive phosphorus. The sample is needed to be acid hydrolysed to convert it into an orthophosphoric form. 100 mL of sample was taken. 50µL of phenolphthalein indicator was added to each 100mL sample. If the red colour was developed, a strong acid solution was poured dropwise to just discharge the colour. Added 1mL H_2SO_4 solution and solution boiled for 90 minutes on a hot plate. The volume of the wastewater was allowed to remain between 25 to 50mL. After boiling the sample was cooled to room temperature and titrated against NaOH and H_2SO_4 until the faint pink colour was achieved. The volume was then maintained at 100mL. 25 mL of the sample was taken and analysed as stated above. A strong acid solution was prepared for the acid hydrolysis of the wastewater. The solution was made by adding 30mL of concentrated sulfuric acid (H_2SO_4 98% pure) to 60mL of distilled water. Added 0.4mL of nitric acid (HNO_3) in the solution and diluted the volume of the solution to 100mL.

3.4.1.3 Analysis for phosphate and heavy metals content

The samples were then analysed using AAS and UV-Vis spectrophotometer for heavy metals and PO_4^{3-} analysis.

3.4.2 Proximate Analysis

The proximate analysis of raw biomass powder, RBC and Fe@BC was conducted to examine the moisture content, volatile matter, ash, and fixed carbon content as per ASTM standard methods (ASTM D5865–13). It entails evaluating a material's principal components, which are often stated as a percentage of the overall weight. Proximate analysis typically examines four major components:

3.4.2.1   Moisture Content:

This metric quantifies the amount of water in a material.

3.4.2.2   *Ash content:*

The inorganic mineral content of a material that remains after full combustion is represented as ash content. It is a critical metric in the examination of organic materials including biochar.

3.4.2.3   *Volatile Matter:*

The fraction of a substance that is lost when heated to a high temperature in a controlled atmosphere. It consists of chemicals such as volatile hydrocarbons and other organic molecules. Volatile matter can indicate how easily a material will combust.

3.4.2.4   *Fixed Carbon*

Fixed carbon is the carbon content that remains after moisture, volatile matter, and ash have been removed. It is a critical parameter for determining the energy content of materials, including biochar.

3.1.1   Point of Zero Charge

The point of zero charge (pHpzc) of biochar obtained from different biomasses will be measured using potentiometric titration method as described by (Bakatula et al., 2018). In this method, 0.2 g of biochar will be added to 40.0 mL of 0.1 M NaNO3 solution in a series of 50 mL conical flasks. The pH adjustment will be done using 0.1 M HNO3 and 0.1 M NaOH solutions, to obtain the initial pH range of 2 to 10 ($\pm$ 0.1 pH units) and denoted as pHi. The samples will be shaken for 24 h using shaker at 200 rpm. After settling, the final pH in each flask will be measured and denoted as pHf. The pHpzc will be obtained from the plot of ΔpH (= pHf – pHi) versus pHi.

3.1.2   Analytical Procedures

The surface morphology and elemental composition of RBC and Fe@BC was examined by an SEM-EDX analyzer (JSM-6490A of JEOL, Japan). The functional groups of RBC, Fe@BC, and AR: Fe@BC (Fe@BC after PO_4^{3-} adsorption) were analyzed through FT-IR (Agilent Cary 630 FTIR Spectrometer (Agilent, USA). X-ray diffraction analysis was performed using the XRD Bruker D8 Advanced X-ray diffractometer (Bruker, Germany) to determine the crystallographic structure of RBC, Fe@BC, and AR: Fe@BC.

3.2 Soil testing and lab scale potting test

Soil was collected from the nursery of National University of Sciences and Technology H-12, Islamabad and then sieved through a screen of 2 mm. PO_4^{3-} and heavy metals content were analysed using AAS and UV visible spectrophotometer. Furthermore, moisture content, pH, electrical conductivity, and water holding capacity of the soil were also determined as per standard procedure (Estefan et al., 2013). The detailed procedure is as follows:

3.2.1　pH

50 grams of air-dried soil (2 mm) were weighed and placed in a 100-milliliter glass beaker for soil analysis. The mixture was then agitated and allowed to stand for 30 minutes, with occasional stirring, after which 50 milliliters of distilled water was added.

The pH meter was calibrated after 30 minutes, and the combination electrode was immersed in the suspension for 30 seconds. The final pH value was 8.06. The electrodes were then cleaned with distilled water and dried.

3.2.2　Electrical Conductivity

Weighing 50 grams of air-dry soil (2 mm) into a 100-mL glass beaker and adding 50 mL of distilled water was the soil analysis process. The suspension was filtered using suction through a readied Buchner funnel with wet Whatman No. 42 filter paper after complete mixing and a 30-minute resting time with intermittent stirring.

The conductivity meter was calibrated when the filtration was finished, and the clear filtrate was transferred to a 50-mL beaker. The conductivity cell was immersed in the solution, and the EC measurement of 4.38 dS/m was recorded. The conductivity cell was cleaned and dried with a tissue after the measurement.

3.2.3　Water Holding Capacity

To prepare the soil sample, it was properly air-dried. A funnel was constructed with tubing attached and filter paper inserted. The 100 mL soil sample was poured into the funnel without being compacted. 100 mL of water was gradually measured and added to the soil. Water was added until the soil got fully saturated. Afterwards clamp was released, and extra water was collected in the graduated cylinder (water drained, mL). The volume of water in the cylinder was measured. Water holding capacity was then calculated by the following equations:

$$: \frac{\text{Water retained (mL)}}{100 \text{ mL sample}} = \text{Water added (mL)} - \text{Water drained (mL)} \tag{10}$$

Water holding capacity was found to be 1.74 in/ft of soil.

3.2.4 Moisture Content

10 g of air-dry soil with particles smaller than 2 mm was weighed and placed in a crucible with a lid that had previously been dried and weighed at 105°C. The soil-filled crucible was then placed in an oven, and dried overnight at 105°C, for 24 hours. The crucible was gently taken from the oven the next day, after the soil had properly dried. The container was fitted with a lid and allowed to cool in a desiccator for at least 30 minutes. Finally, the container was re-weighed to calculate the dry soil sample's ultimate weight.

$$Soil\ Moisture\ (\theta) = \frac{Wet\ soil(g) - Dry\ soil\ (g)}{Dry\ Soil\ (g)} \tag{11}$$

$$Dry\ Soil\ (g) = \frac{1}{1 + \frac{\theta}{100}} \times Wet\ soil \tag{12}$$

$$Moisture\ Factor = \frac{Wet\ Soil(g)}{Dry\ Soil\ (g)}$$

(13)

Moisture content of Sun dried and sieved soil was found to be 0.76%.

3.2.5 Potting test

Pots with the soil capacity of 100g were used to conduct lab scale potting test. Soil was mixed with different composite materials (raw powders, RBC, Fe@BC, and AR: Fe@BC) in 100:2 while keeping pure soil as control. 20 mustard seeds were planted per pot and allowed to grow for six weeks. Afterwards, average root and shoot length, fresh and dry weight of each plant was reported to access the most favourable composite material as fertilizer for plant growth.

<div align="right">

Chapter 4

</div>

RESULTS AND DISCUSSION

4.1 Characterization of raw and Fe-modified biochar

4.1.1 Heavy metals and PO_4^{3-} content

Heavy metals (Zn, Cd, Cr, Pb, Na, K, Fe) and PO_4^{3-} content was analysed for raw powders, RBC and Fe@BC (**Table 1**). The heavy metal content was found much higher in raw powders and decreased in an order raw powder> RBC> Fe@BC. These analysis results suggested that pyrolysis decreases the bioavailability of heavy metals contained in raw material (D. Li et al., 2022). The results indicated most of the heavy metals were found within safe limits as prescribed by WHO. However, higher Cd content in raw powders (2 mg/Kg) and RBC (1 mg/Kg) was observed exceeding permissible level of 0.5 mg/Kg (Ediene & Umoetok, 2017) . In contrast, only higher Fe content was observed in Fe@BC, which may be attributable to $FeCl_3.6H_2O$ based BC activation. The results of PO_4^{3-} content in these materials showed a similar pattern. The heavy metal and PO_4^{3-} content were also analyzed for soil sample (**Table 1**). The results indicated higher concentration of Cd (513 mg/Kg) while it indicated deficiency of essential plant nutrients mainly Fe (1974 mg/Kg) and PO_4^{3-} (408 mg/Kg) (Ediene & Umoetok, 2017; Mengel, 2001). These results suggested the application of micro and macro nutrients in such soil, which may be addressed by recovering orthophosphate from contaminated water using Fe@BC.

Table 2 Physicochemical characteristics of soil, raw powders, RBC and Fe@BC

Material	Proximate analysis					Heavy metals content							
	Moisture (%)	VM (%)	Ash (%)	FC (%)	pH_{PZC}	PO_4^{3-} (mg/Kg)	Na (mg/Kg)	Zn (mg/Kg)	K (mg/Kg)	Pb (mg/Kg)	Cd (mg/Kg)	Fe (mg/Kg)	Cr (mg/Kg)
Raw wheat powder	5.89	69.73	7.64	22.63	-	592.00	238.00	9.00	91.00	4.00	2.00	34.40	N. D
Raw sewage powder	77.8	33.95	37.82	28.23	-	1153.00	232.00	8.00	3.00	3.00	1.00	3862.00	N. D
Raw 5050 powder	55.98	62.00	18.54	19.46	-	380.00	220.00	5.00	66.00	2.00	1.00	1941.00	N. D
WBC	0.98	27.10	20.00	52.90	7.45	154.00	241.00	9.00	13.00	2.00	1.00	29.30	N. D
SBC	0.88	16.68	4.72	78.60	8.56	108.40	247.00	6.00	207.00	1.00	1.00	3300.00	N. D
CBC	0.91	20.89	16.43	62.68	7.93	26.80	239.00	6.00	64.00	1.00	1.00	1645.00	N. D
Fe@WBC	1.21	6.98	1.93	91.09	7.76	84.00	N. D	N. D	N. D	N. D	N. D	131000.00	N. D
Fe@SBC	1.08	4.88	1.47	93.65	8.83	590.00	N. D	N. D	N. D	N. D	N. D	278000.00	N. D
Fe@CBC	1.19	5.74	1.62	92.64	9.82	68.60	N. D	N. D	N. D	N. D	N. D	197000.00	N. D
Soil	-	-	-	-	-	408.00	1700.00	1.00	2000.00	164.00	513.00	1974.00	145.00

4.1.2 Proximate Analysis

The proximate analysis of raw biomass powder, RBC and Fe@BC was conducted to examine the moisture content, volatile matter, ash, and fixed carbon content (Table 2). Moisture content of raw powders was observed to be 5.89 %, 77.8 % and 55.98 % for WSP, SSP and WSP: SSP, respectively. A significant decrease in moisture content was observed after pyrolysis of raw powder and reached to 0.98 %, 0.88 % and 0.91 % for WBC, SBC, and CBC, respectively. Similar trend was also observed by (Jing et al., 2020). However, slight increase in the moisture content of Fe@WBC (1.21 %), Fe@SBC (1.08 %) and Fe@CBC (1.19 %) was observed, which may be attributed to frequent washing of biochars during modification. The results also indicated that the volatile matter and ash content was found to be (69.73 %, 33.95 % and 62 %) and (7.64 %, 37.82 % and 18.54 %) for WSP, SSP and WSP: SSP, respectively. After pyrolysis of raw powders, the volatile matter and ash content significantly decreased and followed the trend as WBC > CBC > SBC, respectively. This trend can be linked to the breakdown of complex organic molecules at high pyrolysis temperatures, resulting in the loss of volatile organic components and the release of volatile gases, as well as an increase in the porosity of the biochar material (Cao et al., 2019; Dutta et al., 2017). Similar observation was observed after modification with $FeCl_3.6H_2O$, which presented volatile combustible matter and ash content as (6.98 %, 4.88 % and 5.74 %) and (1.93 %, 1.47 % and 1.62 %) for Fe@WBC, Fe@SBC and Fe@CBC, respectively. In contrast, the fixed carbon content increased in the order Fe@BC > RBC > raw powders, which may be related to the removal of volatiles and the degradation of organics in the case of RBC and Fe@BC (Cao et al., 2019).

4.1.3 Point of Zero Charge

Point of zero charge (pH_{PZC}) determines the pH at which surface of RBC and Fe@BC has no net electrical charge (Mukherjee et al., 2011). It is an important parameter for understanding the surface chemistry of materials. The point of zero charge (pHpzc) of biochar obtained from different biomasses will be measured using potentiometric titration method. In this method, 0.2 g of biochar will be added to 40.0 mL of 0.1 M $NaNO_3$ solution in a series of 50 mL conical flasks. The pH adjustment will be done using 0.1 M HNO_3 and 0.1 M NaOH solutions, to obtain the initial pH range of 2 to 10 ($\pm$ 0.1 pH units) and denoted as pHi. The samples will be shaken for 24 h using shaker at 200 rpm. After settling, the final pH in each flask will be measured and denoted as pHf. The pHpzc will be obtained from the plot of ΔpH (= pHf – pHi) versus pHi.

It was observed that the pH_{PZC} for WBC, SBC, and CBC (7.45, 8.56, and 7.93) increased to (7.76, 8.83, 9.82) for Fe@WBC, Fe@SBC and Fe@CBC, respectively (**Table 2**). Such observation is consistent with previously reported (S. Wang et al., 2015) which showed an increase in the amount of positive surface charge because of iron impregnation on the biochars' surface will increase the anion exchange capacity and enhanced the redox performance of Fe@BC for our targeted contaminant i.e., PO_4^{-3} from aqueous solution (Lee et al., 2022; Tang et al., 2019).

4.1.4 Speciation Diagram

Speciation diagram for PO_4^{3-} was obtained using Visual MINTEQ.
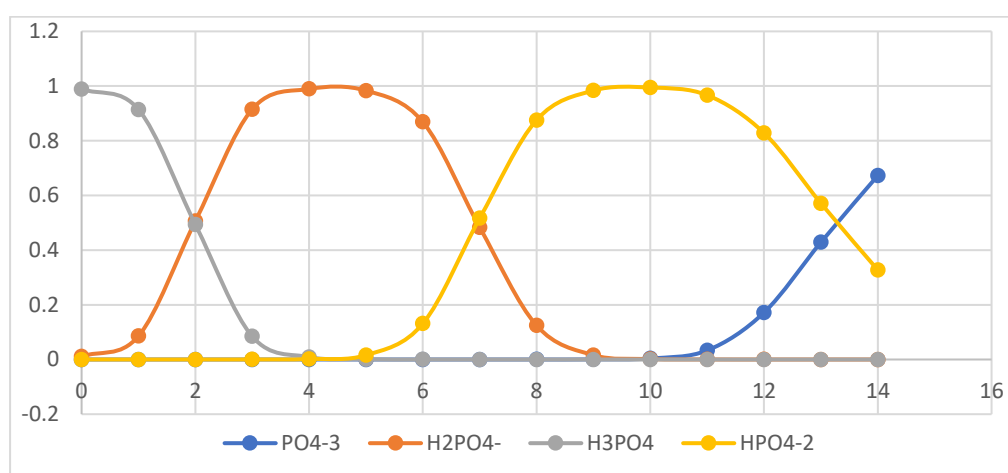
Figure 2 Speciation diagram for PO_4^{3-}

4.1.5 SEM-EDX analysis

SEM-EDX analysis was performed to determine the surface morphology and elemental composition of RBC and Fe@BC.As shown in Figure 3(A, B, C), SBC and CBC presented highly amorphous and porous structure as compared to WBC, which showed uniform structure with vertical tubes. Such variations in structural features of RBC may be attributable to the loss of volatile components at higher pyrolysis temperature. This might result in improvement of surface area, roughness, porosity, and active sites, thus leading to enhanced active sorption sites (Ahmed et al., 2020). After coprecipitation with Fe salt, Fe@WBC presented skeleton type structure with varying pore volume and cracks, while Fe@SBC and Fe@CBC showed irregular and rod like structure with increased porosity (Figure 3(D, E, F)).
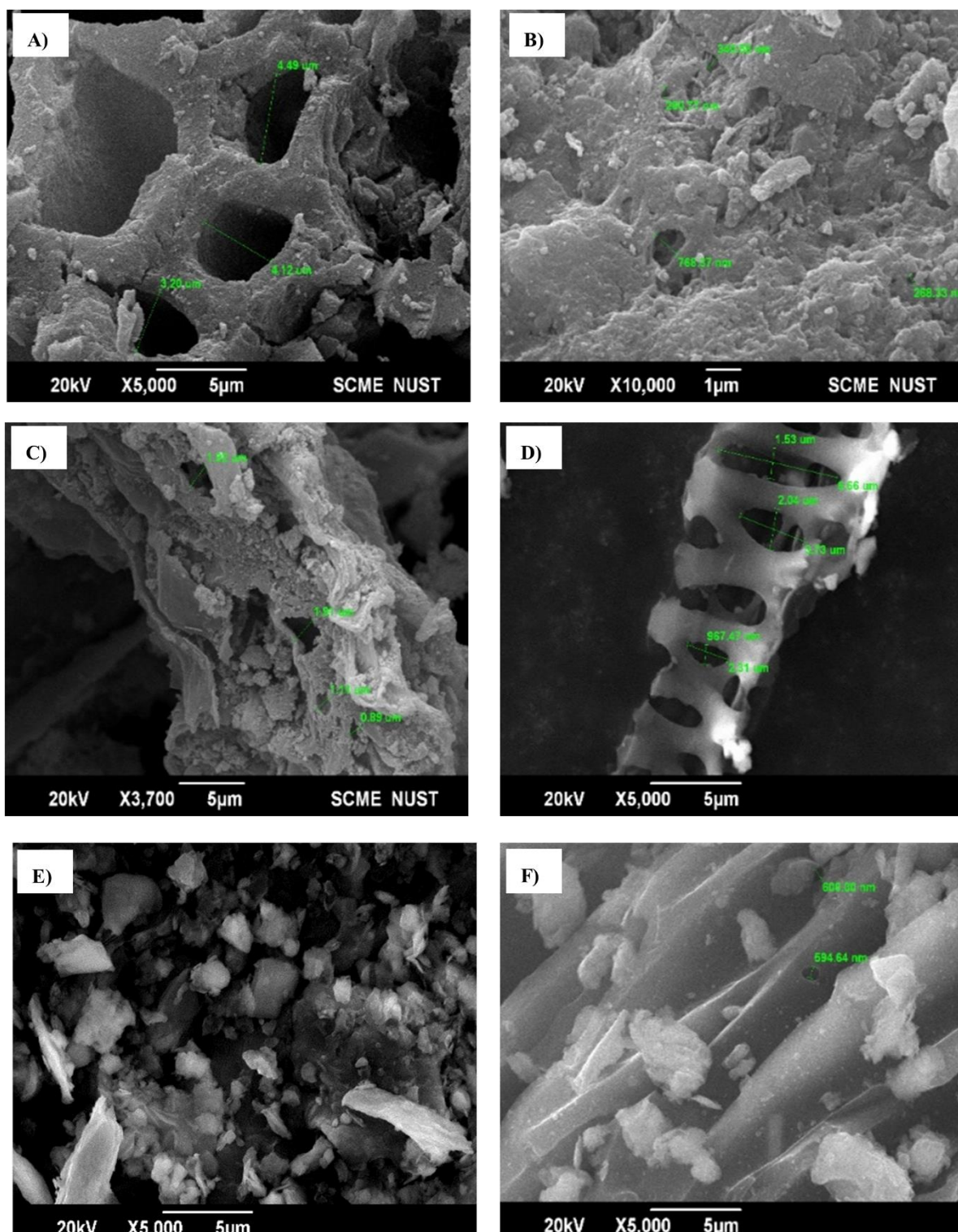
Figure 3 SEM images of different BC presented as **(A)** WBC, **(B)** SBC and **(C)** CBC, **(D)** Fe@WBC, **(E)** Fe@SBC and **(F)** Fe@CBC.

EDX analysis of RBC is presented in Table 3. Fe content was found to be (0%, 2.9% and 0.9%) for WBC, SBC, and CBC.

Table 3 EDX Analysis of RBC

WBC		SBC		CBC	
Element	Weight %	Element	Weight %	Element	Weight %
C K	81.6	C K	0.1	C K	65.7
O K	13.5	O K	56.7	O K	24.1
Na K	0.6	Mg K	0.8	Na K	0.4
Mg K	0.1	Al K	7.9	Mg K	0.3
Si K	0.7	Si K	26.0	Al K	1.0
Cl K	0.7	K K	2.0	Si K	3.4
K K	1.8	Fe K	2.9	Fe K	0.9

However, Fe content significantly increased to (13.1%, 27.8% and 19.7%) for Fe@WBC, Fe@SBC, and Fe@CBC respectively (Table 4). This large increase in Fe content suggests that the activation process was successful in increasing the Fe content in these materials, which is an important indicator of their successful activation for the intended purpose.

Table 4 EDX Analysis of Fe@BC

Fe@WBC		Fe@SBC		Fe@CBC	
Element	Weight %	Element	Weight %	Element	Weight %
C K	65.5	C K	0.0	C K	17.2
O K	13.3	O K	39.1	O K	35.9
Al K	0.2	Al K	3.2	Mg K	1.0
Cl K	0.9	Si K	40.6	Al K	2.6
K K	1.6	K K	1.1	Si K	12.6
Fe K	14.5	Ca K	0.8	K K	0.7
Co K	0.7	Fe K	14.6	Ca K	1.1

4.1.6 FT-IR and XRD analysis

The FT-IR spectra of RBC and iron-modified biochar (Fe@BC) are presented in Figure 4(A, B), illustrating noticeable shifts in the peaks. In WBC, peaks at at ~ 3620 cm^{-1}, 2070 cm^{-1}, 1558 cm^{-1}, 1363 cm^{-1}, 1023 cm^{-1} and 865 cm^{-1} in WBC shifted to ~3621 cm^{-1}, 2079 cm^{-1}, 1562 cm^{-1}, 1374 cm^{-1}, 1027 cm^{-1} and 872 cm^{-1}, respectively in Fe@WBC (Figure 2(A, B)). Similarly, shift in peaks in SBC and Fe@SBC was observed, confirming that Fe species form complexes with various functional groups present on BC surface (Figure 4(A, B))(R. He et al., 2019). Moreover, new peak observed at ~3383 cm^{-1} in Fe@CBC indicates the formation of Fe-OH complexes on CBC surface, which may be responsible for enhancement in its surface characteristics (Jiang et al., 2016). These observations suggest

successful modification of Fe due to strong Fe-BC complexation reactions. The observed shifts indicate altered molecular interactions resulting from the introduction of Fe species onto the BC surface (R. He et al., 2019). The shift in peaks observed in the Fe@BC indicates an enhanced binding affinity and increased adsorption potential, particularly for PO_4^{3-} ions. These spectral changes provide evidence of the successful modification of the BC surface with Fe, which may result in improved PO_4^{3-} sorption performance.
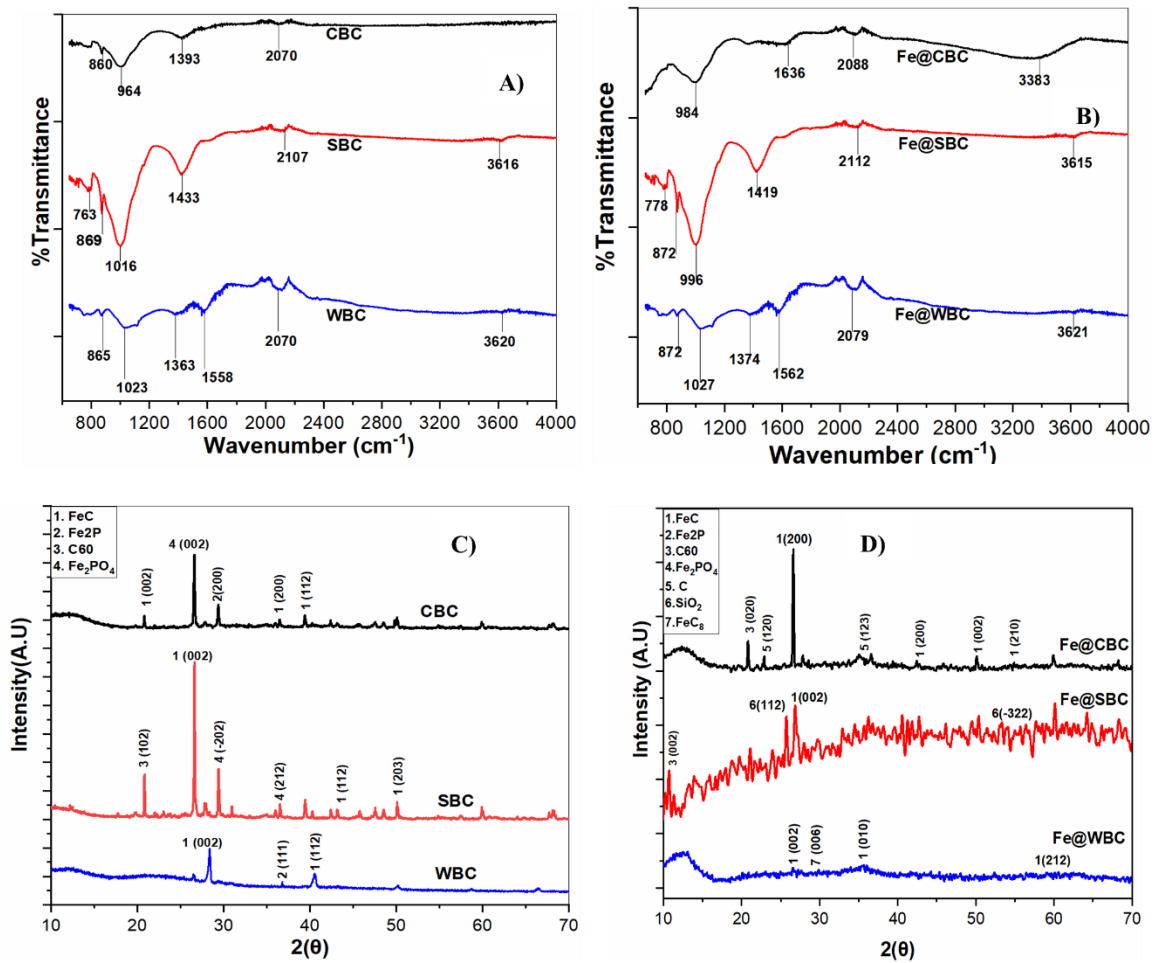
Figure 4 (A, B) FT-IR and **(C, D)** XRD spectra of RBC and Fe@BC.

The XRD spectra of RBC and Fe@BC is presented in **Figure 4(C, D)**. The diffraction peaks of FeC were detected at 2θ values of 26.426° and 50.373° for WBC which were ascribed orthorhombic structures, respectively (PDF# 030411) (D. Liu et al., 2018). The FeC peaks were also observed at 26.426°, 35.891° and 62.268° for Fe@WBC and associated with orthorhombic structures, respectively. Fe_2P peak was found at 40.283° for WBC, which was associated to hexagonal structures (PDF# 271171). Furthermore, peak of FeC_8 was also observed at 28.217° for Fe@WBC, which were related to monoclinic structure (PDF# 510624). Similarly, FeC peaks were observed at (SBC: 26.426°, 42.193° and 50.373°) and

(Fe@SBC: 26.426°), that attributed to orthorhombic structure, respectively (D. Liu et al., 2018). Moreover, C_{60} peak was found as SBC: 23.371° and Fe@SBC: 10.870°, attributed to orthorhombic structure (PDF#491718). In addition, $Fe_3(PO_4)_2$ peaks were found as (SBC: 33.024° and 39.589°) were linked to monoclinic structure (PDF#491087) (Sun et al., 2019). However, SiO_2 peaks were observed as (Fe@SBC: 26.749° and 51.626°) and were ascribed to monoclinic structure (PDF#461441). In case of CBC and Fe@CBC, FeC peaks were observed at (42.193° and 50.373°) and (26.426°, 42,193°, 50.373° and 54.321°), attributed to orthorhombic structure respectively. The diffraction bands in CBC at 35.307° and 29.491° of Fe_2PO_4 correspond to hexagonal structure and monoclinic structure, respectively. A new C peak in Fe@CBC appeared at 22.765° and 34.222° were linked with hexagonal structure, respectively while C_{60} peak found at 20.034° was associated with orthorhombic structure (PDF #491087). These XRD results indicated appearance of new peaks as (Fe@WBC: FeC_8), (Fe@SBC: SiO_2) and (Fe@CBC: C). Moreover, broadening and narrowing of FeC peaks were observed in Fe@CBC and Fe@SBC, respectively. The degree of crystallinity of all sorbents i.e., Fe@WBC, Fe@SBC and Fe@CBC were calculated to be as 17.5%, 11.5% and 8.8%, respectively. This implies that Fe modification influences the surface porosity, structure, and roughness of synthesized BC (Zeng & Kan, 2022).

4.2 Effect of Fe@BC dosage and pH

As shown in Figure 5(A), at 0.1 g/L Fe@WBC, Fe@SBC and Fe@CBC, the PO_4^{-3} removal potential (0.16 %, 24 % and 27 %) and adsorption capacity (0.l6 mg/g, 24.8 mg/g, and 27.3 mg/g), respectively was observed. The low sorption capacity may be due to the limited adsorption sites at lower Fe@BC dosages (Li et al., 2019). Upon increasing Fe@BC dosages up to 5 g/L, the PO_4^{-3} sorption potential (83.5%, 100% and 100%) and adsorption capacity (1.67 mg/g, 2.071 mg/g, and 2.072 mg/g) was achieved. This suggests positive correlation between number of adsorption sites and added amount of Fe@BC dosage. Similar behavior was also observed by (Deng et al., 2021), where increased BC dosages enhanced the PO_4^{3-} removal from contaminated water. Considering removal potential (43.25%, 86.5% and 87.05%) and sorption capacity (2.16 mg/g, 4.3 mg/g, and 4.4 mg/g) of respective BC for PO_4^{-3}, 2g/L Fe@BC dosage was selected for subsequent experiments.
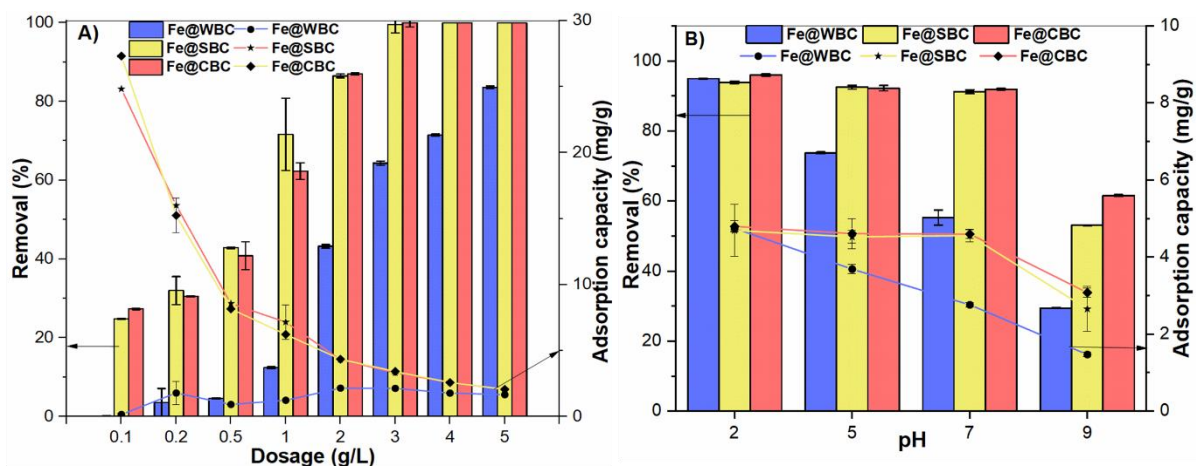
Figure 5 Effect of **(A)** Fe@BC dosages and, **(B)** solution pH on PO_4^{-3} removal

The experiments were also conducted by varying pH values from 2 to 9 to monitor PO_4^{3-} removal using Fe@BC (Figure 5(B)). The results indicated that at acidic pH 2, the Fe@WBC, Fe@SBC and Fe@CBC presented greater PO_4^{-3} removal potential (94.9%, 93.88% and 95.96%) and maximum adsorption capacity (4.75 mg/g, 4.69 mg/g, and 4.8 mg/g), respectively. Such excellent performance may be related to the presence of Fe@BC with net positive surface charge and neutral $H_3PO_4^0$ and anionic H_2PO_4- species at extremely acidic conditions. Upon increasing pH to 5 and 7, the PO_4^{-3} removal potential of Fe@WBC, Fe@SBC and Fe@CBC decreased to (73.75%, 92.50% and 92.21%) and (55.25%, 91.21%, 91.93%), respectively. However, the significant decrease in PO_4^{-3} removal potential (29.41%, 53.08% and 61.58%) and adsorption capacity (1.47 mg/g, 2.65 mg/g, and 3.1 mg/g), respectively of Fe@WBC, Fe@SBC and Fe@CBC was observed at pH 9. Such observation may be related to the electrostatic repulsion between anionic Fe@BC and negatively charged HPO_4^{-2} at alkaline pH. Similar results were reported by (Huang et al., 2020a) which showed significant reduction in PO_4^{-3} removal with increasing pH values. We selected pH 7 for subsequent experiments since Fe@BC was intended to be used as a fertilizer material.

4.3 Kinetic study

The results of kinetics study showed that Fe@WBC, Fe@SBC, and Fe@CBC presented PO_4^{-3} removal potential 16.13%, 59.95% and 63.8%, respectively at reaction time of 15 min (Figure 6A). As the reaction time increases from 30 min to 180 min, sorption potential of Fe@WBC, Fe@SBC and Fe@CBC increased from (25.08%, 67.33% and 65.67%) to (55.25%, 91.21% and 91.93), respectively. Similar results were reported in previous study (Almasri et al., 2019). Upon further increasing reaction time up to 480 min, insignificant

increase in PO_4^{-3} removal was observed. Therefore, optimum reaction time of 180 min was selected for subsequent experiments.

The results also indicated that adsorption capacity increases for each Fe@BC upon increasing reaction time (Figure 6B). For instance, at 15 min, adsorption capacity of Fe@WBC, Fe@SBC and Fe@CBC for PO_4^{-3} was observed to be 0.81 mg/g, 2.99 mg/g, and 3.19 mg/g, respectively. It increased to 3.05 mg/g, 5.05 mg/g, and 4.99 mg/g for reaction time of 480 min. Moreover, kinetic specifications and fitting of PO_4^{-3} sorption data by Pseudo first order (PFO) and Pseudo second order (PSO) models are presented in Figure 6B. The PSO model was better fitted for kinetics data as indicated by regression coefficients: R^2 (Fe@WBC: 0.982; Fe@SBC: 0.958 and Fe@CBC: 0.986) when compared with PFO model coefficients (Fe@WBC: 0.964; Fe@SBC: 0.896 and Fe@CBC: 0.947) (Table 5). This suggests the dominant role of chemisorption process using Fe@BC for PO_4^{-3} removal from water (Salim et al., 2021).

Table 5 Kinetic Models

Model	PSO		
Equation	$Q_t=(k_2*t*q_e^2)/(1+k_2*q_e*t)$		
Plot	Fe@WBC	Fe@SBC	Fe@CBC
qe	3.47022 +/- 0.15909	4.74901+- 0.19248	4.76242+- 0.1074
K_2	0.00478 +/- 8.97	0.01754+/- 0.00469	0.2246+/- 0.00371
Reduced Chi	0.01871	0.09527	0.03295
R-square(corrected)	0.98419	0.96337	0.98734
Adjusted R-square	0.98193	0.95813	0.98553
Model	PFO		
Equation	$Q_t=q_e-(exp(ln(q_e)-k_1*t))$		
Plot	Fe@WBC	Fe@SBC	Fe@CBC
qe	2.95466+/- 0.14264	4.37192+/ 0.20798	4.47803+/-0.1455
K_1	0.01374+/-0.00193	0.06042+/-0.01507	0.06449+/-0.01192
Reduced Chi	0.03726	0.23522	0.11888
R-square(corrected)	0.96851	0.90955	0.95432
Adjusted R-square	0.96401	0.89663	0.94779
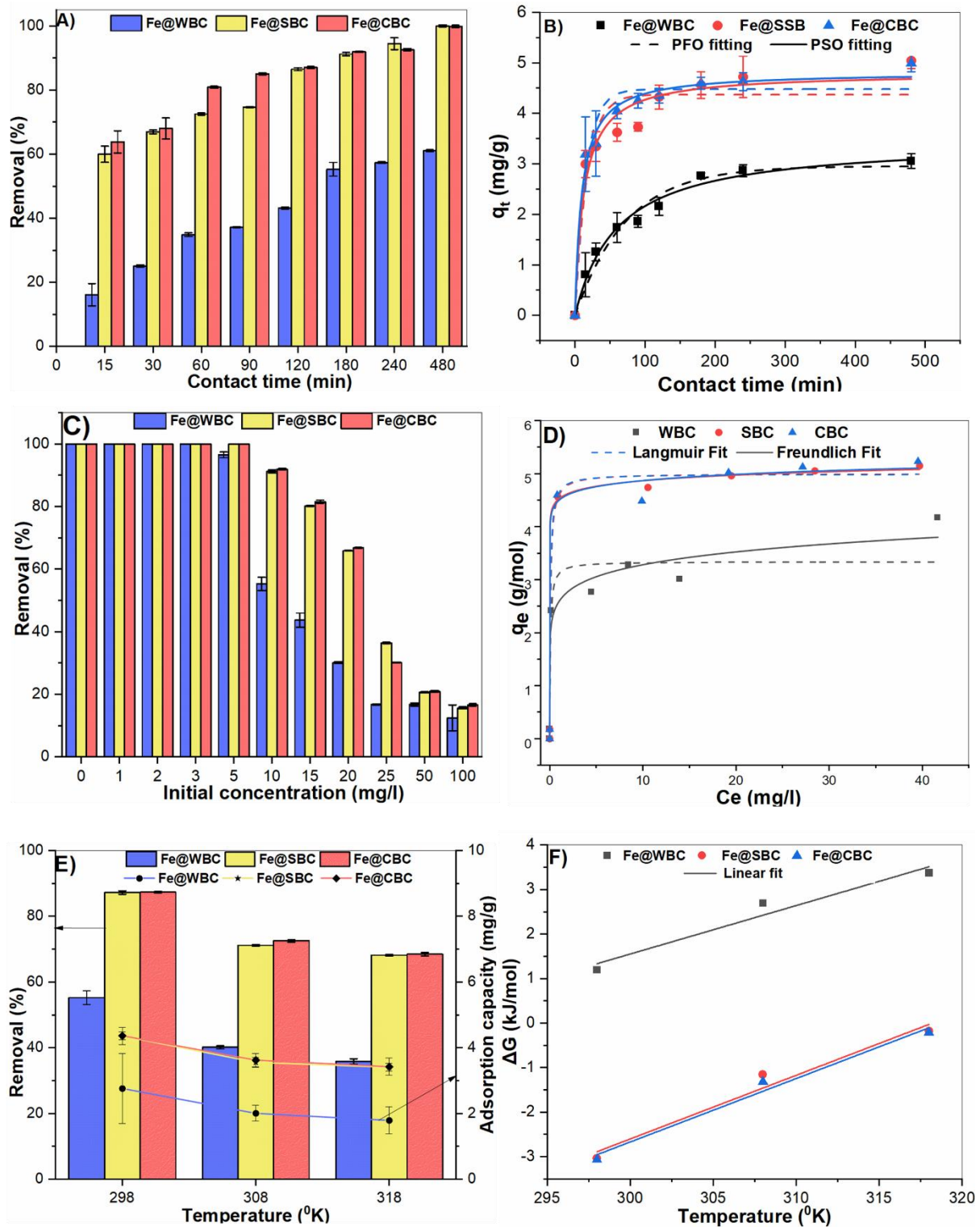
Figure 6 Figure 4 showing **(A)** effect of contact time on PO_4^{-3} removal; **(B)** adsorption kinetics; **(C)** effect of initial concentration on PO_4^{-3} removal; **(D)** adsorption isotherms; **(E)** Effect of suspension temperature on PO_4^{-3} removal performance and; (F) adsorption

4.4 Isotherm study

Figure 6(C) presents PO_4^{3-} sorption potential of Fe@BC as a function of initial PO_4^{3-} concentration. The results indicated a significant decline in PO_4^{3-} removal from 100% to

(16.68%, 20.59% and 20.93%) of Fe@WBC, Fe@SBC, and Fe@CBC, respectively. These results are in good agreement with previous study (Huang et al., 2020b), which showed negative effect on removal performance with increasing PO_4^{-3} concentration using modified biochar. The experimental data was fitted with the two most used sorption isotherms i.e., Langmuir and Freundlich (Figure 6(D)). Freundlich model was better fitted, as indicated by higher R^2 values (Fe@WBC: 0.964; Fe@SBC: 0.998 and Fe@CBC: 0.992) when compared with Langmuir model coefficients (Fe@WBC: 0.991; Fe@SBC: 0.996 and Fe@CBC: 0.988) (Table 6). The R^2 values suggested that sorption of PO_4^{-3} by Fe@BC followed Freundlich model and is not limited to a fixed number of adsorption sites (Khayyun & Mseer, 2019).

Table 6 Isotherm Models

Model	Langmuir		
Equation	$q_e=(qm*k*C_e)/(1+k*C_e)$		
Plot	Fe@WBC	Fe@SBC	Fe@CBC
q_m	3.33954 +/- 0.2439	5.034 +/- 0.078	4.99336+/- 0.1385
kL	13.98665 +/-10.45	11.28693 +/-4.67	13.19097 +/- 10.19
Reduced	0.22096	0.02207	0.06845
R-square	0.9261	0.99668	0.98975
Adjusted R-square	0.91132	0.99601	0.9877
Model	Freundlich		
Equation	: $q_e= k*(C_e^{(1/n)})$		
Plot	Fe@WBC	Fe@SBC	Fe@CBC
Kf	2.59052+/- 0.195	4.52899+/- 0.0985	4.4981+/- 0.18866
n	9.73457+/- 2.677	32.04666+/- 7.846	29.05246 +/- 12.504
Reduced Chi-S	0.08955	0.01158	0.04461
R-square (COD)	0.97005	0.99826	0.99332
Adjusted R-Square	0.96406	0.99791	0.99199

4.5 Thermodynamic study

As presented in **Figure 6(E)**, at 298^0K, the PO_4^{-3} removal potential (55.25%, 87.58% and 87.3%) and adsorption capacity (2.76mg/g, 4.36mg/g and 4.37mg/g) of ^{Fe}@WBC, Fe@SBC, and Fe@CBC, respectively were observed. Upon increasing temperature to 318^0K, the significant decrease in PO_4^{-3} removal potential (35.83%, 68.17% and 68.5%) and adsorption capacity (1.79mg/g, 3.4mg/g and 3.42mg/g) was observed. Similar results were also reported in previous study (Das et al., 2006). Such behaviour may be linked with the increased thermal energy that weakens the bond strength between PO_4^{-3} anions and Fe@BC, thus decreasing removal performance of system (Inam et al., 2021).

Figure 6(F) and Table 7 indicate the thermodynamic parameters calculated using Van't Hoff plot with R^2 values (Fe@WBC: 0.909, Fe@SBC: 0.936 and Fe@CBC: 0.965). The negative values of ΔG at 298 ºK, 308 ºK and 318 ºK (Fe@SBC: -3.04, -1.16 and -0.18

KJ/mol) and (Fe@CBC: -3.06, -1.31 and -0.22 KJ/mol) indicated that the sorption process is spontaneous and energetically favorable (Günay et al., 2007a). In contrast, positive values of Gibbs free energy change (ΔG) i.e., 1.19, 2.69 and 3.37 KJ/mol at respective suspension temperatures were observed for Fe@WBC, thus suggesting non-spontaneous nature of sorption process. The negative enthalpy change (ΔH) values of -31.105, -45.501 and -45.42 KJ/mol for Fe@WBC, Fe@SBC, and Fe@CBC, respectively was observed, which indicated exothermic nature of sorption process (Inam et al., 2021). An earlier study (Günay et al., 2007b) illustrated sorption mechanisms based on ΔH values of 0-8 KJ/mol, 8-60 KJ/mol and > 60 KJ/mol as physisorption, physicochemical sorption and chemisorption, respectively. Since, current study presented modeled ΔH values in the range of 8-60 KJ/mol, therefore, this suggests that removal of PO_4^{-3} anions by Fe@BC is mainly governed by physicochemical sorption mechanisms. In addition, positive entropy change (ΔS) values (Fe@WBC: 0.108 KJ/mol.°K, Fe@SBC: 0.143 KJ/mol.°K and Fe@CBC: 0.143 KJ/mol.°K) indicated increase in surface randomness during PO_4^{-3} removal process. In general, thermodynamic parameters were useful in elucidating the role of Fe@BC heterogeneous surface in eliminating PO_4^{-3} anions from aqueous media during the sorption process.

Table 7 Thermodynamic Models

Equation	Y=a+b*x		
Plot	Fe@WBC	Fe@SBC	Fe@CBC
Weight	No weight		
Intercept (DEL h)	-31.10544	-45.50181	-45.42307
Slope (Del S)	0.10885+/-	0.14299 +/-	0.1425+/-
Residual sum	0.11288	0.13526	0.07193
Pearson R-square	0.977	0.98386	0.99126
R-square ©	0.95453	0.96798	0.9826
Adjusted R-square	0.90906	0.93596	0.9652

4.6.   Effect of interfering species on PO_4^{-3} removal

Figure 7(A, B, C) presents the impact of various anionic species and concentrations on PO_4^{3-} removal using Fe@WBC, Fe@SBC, and Fe@CBC. Cl^- ions at 10mg/L and 50mg/L greatly enhance PO_4^{3-} removal up to 100%, likely ascribed to impurity removal and increased porous surface sites from acidic treatment of Fe@BC (Sahu et al., 2021). Higher Cl^- concentration (100mg/L) reduces PO_4^{3-} removal in Fe@WBC and Fe@CBC (Figure 7 A, C). Fe leaching from BC after acidic treatment causes up to 60% decline in PO_4^{3-} sorption (Shan et al., 2019). PO_4^{3-} sorption with Fe@BC is synergistically enhanced by higher SiO_3^{2-} and HCO_3 concentrations (Figure 7A, B, C). This can be attributed to inner sphere complexation processes, which boost PO_4^{3-} removal from suspension and increase ion pair formation on

Fe@BC (Inam et al., 2018). With Fe@BC, NO3 anions exhibit a competitive inhibition and outer sphere complexation pattern that is PO_4^{3-} removal antagonistic. Due to competition for active sites on the Fe@BC surface, SO_4^{2-} anion reduction of PO_4^{3-} removal capability is substantial (Geelhoed et al., 1997). By creating active surface complexes on Fe@BC and increasing reactivity towards PO_4^{3-} ions, mixed anions increased PO_4^{3-} elimination (Y. Yang et al., 2006). Furthermore, anions stabilize Fe@BC particles, prevent agglomeration, and increase available surface area for PO_4^{3-} adsorption (Alghamdi et al., 2019). PO_4^{3-} ions compete with interfering ions for binding sites on Fe@BC, increasing the amount of PO_4^{3-} that is adsorbed to the surface (Zhu et al., 2008). In general, our results indicate an improved performance of Fe@BC for PO_4^{3-} removal in multicomponent environment.
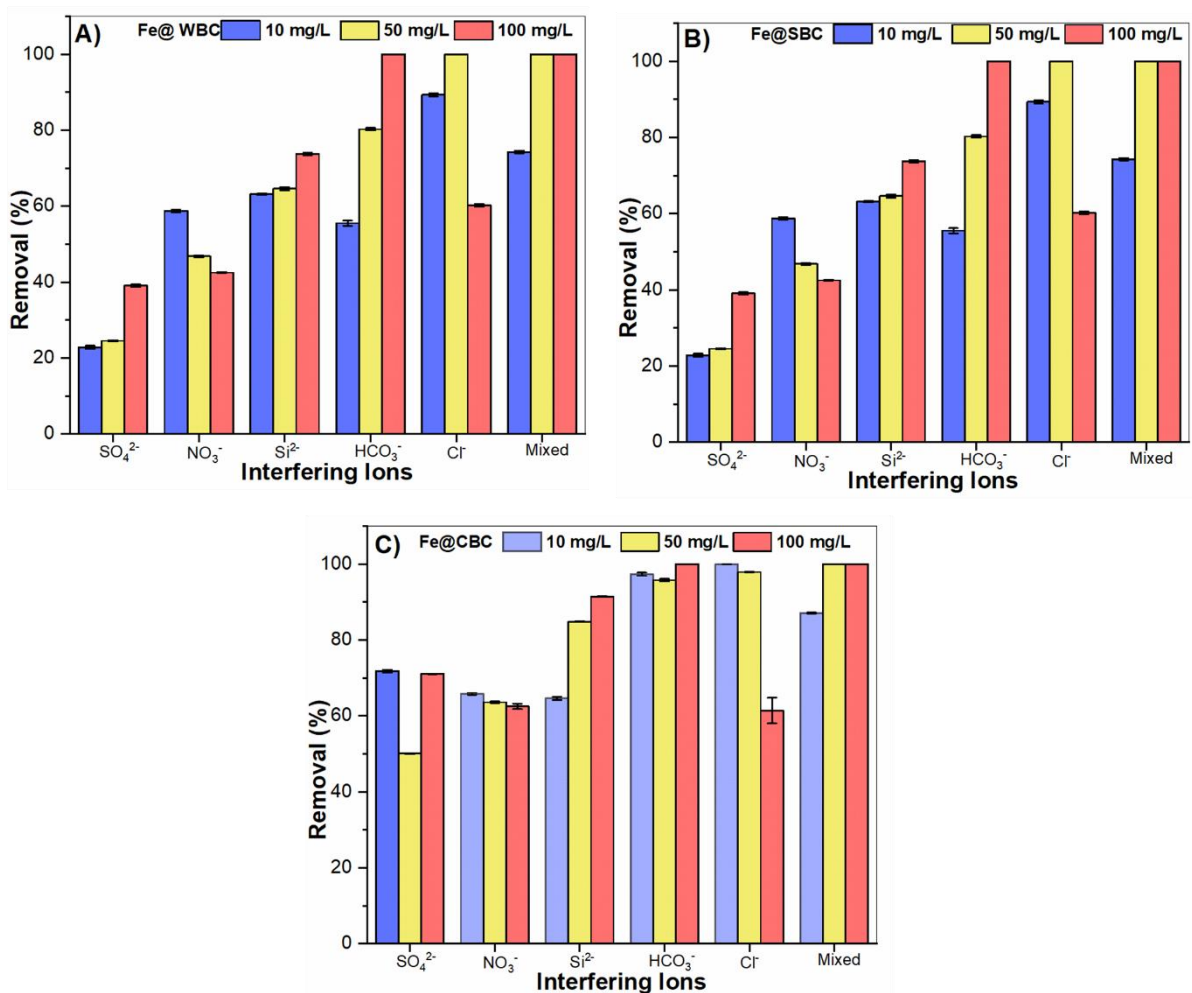
Figure 7 showing effect of interfering species on PO_4^{3-} removal using **(A)** Fe@WBC, **(B)** Fe@SBC and **(C)** Fe@CBC.

4.7. Removal mechanism

The experimental results, mathematical models and spectroscopic techniques were considered to investigate the sorption behaviour of PO_4^{-3} anions using Fe@BC from synthetic

water. Based on experimental results, the influence of various water chemistry parameters on PO_4^{-3} removal performance by Fe@BC was identified.

At acidic pH (2), 3-hour contact time, 25°C suspension temperature, and 2 g/L adsorbent dosage, Fe@BC demonstrated better sorption affinity for PO_4^{-3} anions. Investigations into sorption kinetics, isotherms, and thermodynamics identified multilayered chemisorption and physisorption reactions as the predominant mechanisms. It was discovered that PO_4^{-3} sorption on Fe@BC was exothermic and energetically advantageous, with greater randomness on heterogeneous surface sites. Inner sphere complexation has been proposed as the mechanism for effective PO_4^{-3} elimination by mixed anions. Additional mechanistic insights into the sorption capability of Fe@BC for PO_4^{-3} anions were obtained by FT-IR and XRD studies (Figure 8A). The results of FT-IR analysis in AR: Fe@WBC indicated disappearance, appearance and shifting of different peaks, thus indicating role of various complexation reactions between PO_4^{-3} and Fe@WBC (Figure 8A). S=O group disappearance (1374 cm^{-1}) suggests covalent interaction between S=O and PO_4^{-3} anions on Fe@WBC. Peak shifts (1027-970 cm^{-1}) indicate C-N and C=C vibration changes (Inam et al., 2019). AR: Fe@SBC represents C=C and OH bending peak disappearance, suggesting physisorption (Maugé et al., 2001). New peaks at 1012 cm^{-1} and 1629 cm^{-1} indicate chemical bonding via C-N and C=C stretching vibrations (Inam et al., 2019). No band disappearance in AR: Fe@CBC suggests complexation. Other peak shifts indicate PO_4^{-3} anion-Fe@BC complexation (R. He et al., 2019). Results demonstrate involvement of complexation, physical adsorption, ligand exchange, and chemical bonding in PO_4^{-3} removal by Fe@BC from water. Previous studies have revealed the involvement of similar PO_4^{3-} sorption mechanism (Del Nero et al., 2010; Sabadash et al., 2016)

The XRD results of AR: Fe@BC presented appearance and disappearance of various minerals, showing predominant role of chemical reaction between PO_4^{-3} and Fe@BC (Figure 8B). AR: Fe@WBC demonstrated the disappearance of FeC8 peak ($28.217°$) after PO_4^{-3} adsorption, indicating chemical bonding (J. He et al., 2020). In contrast, three different minerals i.e., FeSiC, C and FePO$_4$ peaks appeared at (12.215^0 and 34.882^0), 13.289^0 and 35.093^0, respectively (PDF# 180651, 501364 and 300659). These peaks corresponded to orthorhombic, tetragonal, and orthorhombic structure, respectively. In comparison, AR; Fe@SBC showed appearance of four different peaks of FePO$_4$ (30.093^0, 20.494^0, 35.093^0, 44.973^0) correspond to orthorhombic structures. Additionally, two new peaks (13.289^0 and 40.283^0) were linked with C and Fe$_2$P and related to tetragonal and hexagonal structure,

respectively. Fe_2P peak appearance suggests electron transfer from Fe@SBC lattice to **PO_4^{-3}** during adsorption, implicating the reduction process. When compared to AR: Fe@SBC and AR: Fe@CBC, C_{60} peaks at 10.870^0 in Fe@SBC and Fe@CBC vanished. SiO_2 peaks in Fe@SBC at 26.749^0 and 51.626^0 disappears in AR: Fe@SBC. Three new C peaks (20.8350, 36.4950, 39.4910) and two new FeP peaks (37.1520, 30.8500) with hexagonal structures both appeared in AR: Fe@CBC spectrum. Both AR: Fe@SBC and AR: Fe@CBC show that PO_4^{-3} reduction and subsequent adsorption are involved. With different intensities, FeC peaks showed consistently in all Fe@BC and AR: Fe@BC samples. The interaction of Fe@BC with PO_4^{-3} anions revealed new peaks ($FePO_4$, Fe_2P and FeP), according to the XRD results. Figure 8C presents the suggested mechanism for PO_4^{-3} adsorption. These findings support the chemical dependence of Fe@BC on feedstock and water properties.

In general, complexation occurs through the formation of bonds between Fe@BC surface and PO_4^{3-}, driven by electrostatic attraction and supported by observable shifts in FT-IR peaks. Physical adsorption, as described by kinetic models (PFO and PSO), is facilitated by weak interactions that occur rapidly due to electrostatic forces and van der Waals interactions. Ligand exchange takes place as functional groups on Fe@BC interact with PO_4^{3-}, resulting in alterations to the functional groups and crystalline structure, as confirmed by FT-IR and XRD data. Chemical bonding involves the formation of either covalent or ionic bonds between Fe@BC and PO_4^{3-}, as verified by FT-IR and XRD analysis. Collectively, these mechanisms contribute to the efficient removal of PO_4^{3-} by Fe@BC.
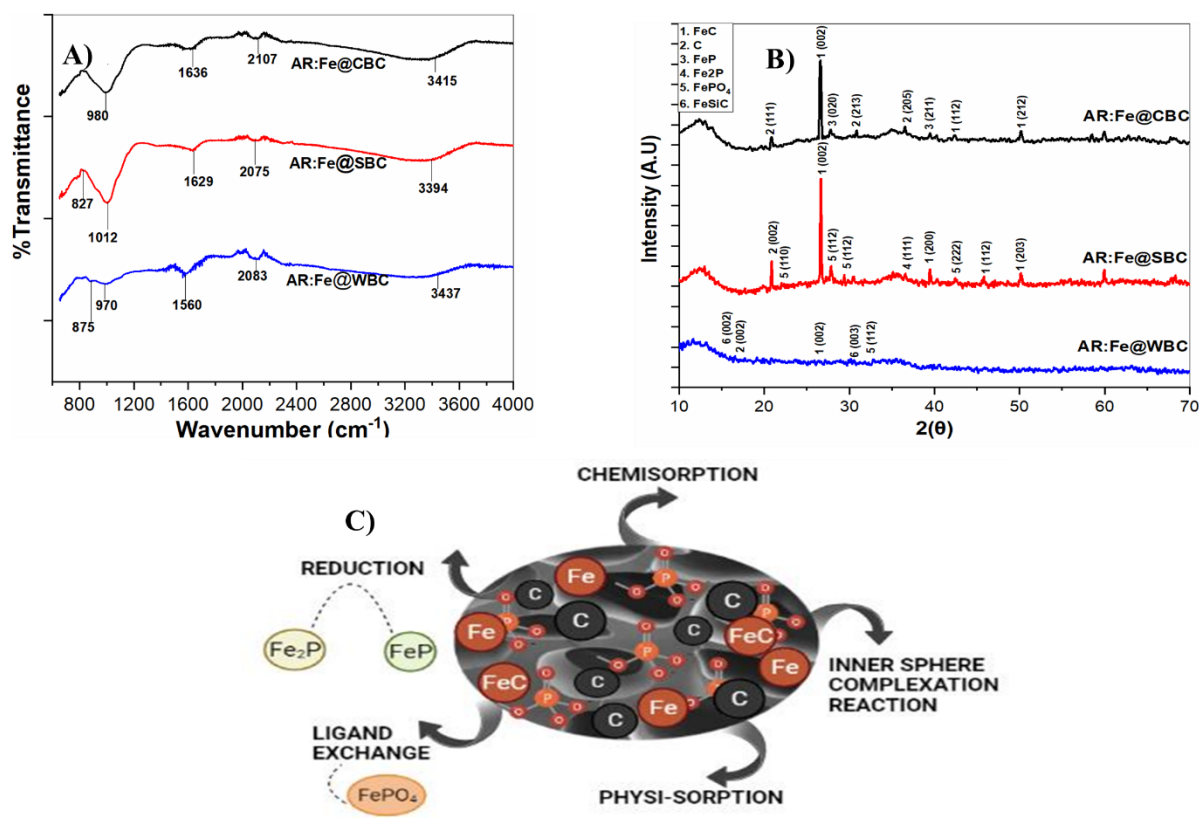
Figure 8 **(A)** FT-IR and **(B)** XRD of AR:Fe@BC; **(C)** Proposed PO_4^{3-} adsorption mechanism after interaction with Fe@BC

4.8.   Application of PO_4^{-3} based Fe@BC as potential fertilizer

Mustard seeds were evaluated (on biomasses, BC, Fe@BC, and PO_4^{-3} sorbed Fe@BC) in lab-sized pots (soil: additive ratio 100:2). Along with pure soil as control, 12 samples were used and the physical characteristics of mustard plants in each situation are shown in Figure 9. The root and shoot lengths of mustard plants varied with AR: Fe@BC > Fe@BC > RBC > Raw powder > Pure soil (0.48 to 2 cm and 5.2 to 9 cm, respectively) (Figure 9A, B). The greatest significant improvement was displayed by AR: Fe@CBC. For spinach, similar outcomes were obtained by Jabborova et al., 2021. Additionally, fresh, and dry weight of mustard plants were also monitored (Figure 9C, D). In comparison to pure soil (64 mg), fresh weight was reduced with various additives (23 to 57 mg). However, compared to pure soil, Fe@CBC, and AR: Fe@BC showed higher fresh weights (72 to 79 mg) (Figure 9C). The dry weight of mustard plants with raw wheat and sewage powder, WBC, and Fe@WBC (4.2-4.7 mg) was lighter than pure soil (5 mg). Other additives had greater dry weight (5.7-8.3 mg) than pure soil (Figure 9D). AR: Fe@CBC exhibited the highest root length (2 cm), shoot

length (9 cm), fresh weight (79 mg), and dry weight (8.3 mg) of mustard plants, indicating strong potential as a phosphatic fertilizer.

4.9. Economic Analysis

This study assessed economic analysis of PO_4^{3-} removal using Fe@CBC. The evaluation considered factors such as the prices of raw materials, production costs, and the subsequent treatment of phosphate-loaded sorbents. Additionally, the disposal of sludge in the sewage treatment plant itself requires financial resources, which could serve as a subsidy for the preparation of sorbents (Li et al., 2019). The subsidy provided for SS disposal in dumpsite could be approximately $40 per metric ton (Li et al., 2023). Moreover, wheat straw is readily available at a very low market price of $0.03 per kilogram. In China, the estimated production cost of biochar was $350 per metric ton in 2021, therefore, biochar production cost was selected accordingly (Shackley et al., 2011). In this evaluation, various factors including protection gas, energy consumption, and manpower were included. Additionally, it was demonstrated that the AR: Fe@CBC have the potential to serve as slow-release PO_4^{3-} fertilizers, therefore, it can be utilized as fertilizer for garden plants, resulting in additional profit as a cost subsidy. The economic analysis aligns with a PO_4^{3-} removal efficiency of over 90%, under the following reaction conditions: an initial PO_4^{3-} concentration of 10 mg/L and Fe@CBC dosage of 2 g/L.

The sludge powder was obtained by washing, dewatering, and crushing the activated sludge. A yield ratio of about 20% (denoted as Y_1) was determined by weighing the mass of sewage sludge and dried sludge powder. Fe@CBC were prepared by co-pyrolysis of the mixture of wheat straw powder and sewage sludge powder and the yield ratio of 55.2% (denoted as Y_2) was determined by weighing the mass of Fe@CBC and their precursors.

The PO_4^{3-} removal efficiency of >90% could be achieved with the initial PO_4^{3-} concentration of 10 mg/L and adsorbent dosage of 2.0 g/L. Therefore, the quantitative relationship between the required absorbent and the corresponding removed PO_4^{3-} is 200 kg adsorbent/kg P. The calculation details of the PO_4^{3-} removal cost are as follows:

➤ The mass of Fe@CBC precursor: (200 kg/kg P)/Y_2 = 200/55.2=3.62kg/kg P;

➤ The required quantities of sludge powder and wheat straw: (3.6 kg/kg P)/2=1.81 kg/kg P (the sludge powder and wheat straw were mixed in a ratio of mass 1:1);

➤ The required quantity of activated sludge: (1.8 kg/kg P)/Y_1 = (1.8 kg/kg P)/0.2 =9.05 kg/kg P;

➤ The cost of activated sludge: 9.05 kg/kg P ´ (-0.04 $/kg) = -0.362 $/kg P;

- The cost of wheat straw: 1.81 kg/kg P ´ ($3´10^{-2}$ \$/kg) = 0.0543\$/kg P;
- Biochar production cost: (200 kg adsorbent/kg P) ´ 0.0543 \$/kg adsorbent = 10.86 \$/kg;
- Saturated biochar: (0.9 kg P + 200 kg adsorbent/kg P) ´ (-0.06\$/kg) = -10.045 \$/kg P

The total cost of PO_4^{3-} removal by Fe@CBC:

[(cost of sewage sludge) + (cost of wheat straw) + (biochar production cost) + (saturated biochar)] = net cost/benefit

[(-0.362) + 0.0543+ 10.86+ (-12.054)] \$/kg P = -1.5\$/kg P

As presented in Table the total profit of PO_4^{3-} removal and recovery using Fe@CBC is estimated to be \$1.5 per Kg.

Table 8 Economic Analysis

Factors	Market price (\$/kg)	PO_4^{3-} removal cost (\$/kg)
Sludge water content (80%)	-0.04	-0.362
Wheat straw	$3x10^{-2}$	0.0543
Biochar production cost	0.35	10.86
Saturated biochar	-0.10	-12.054
Total cost		-1.5
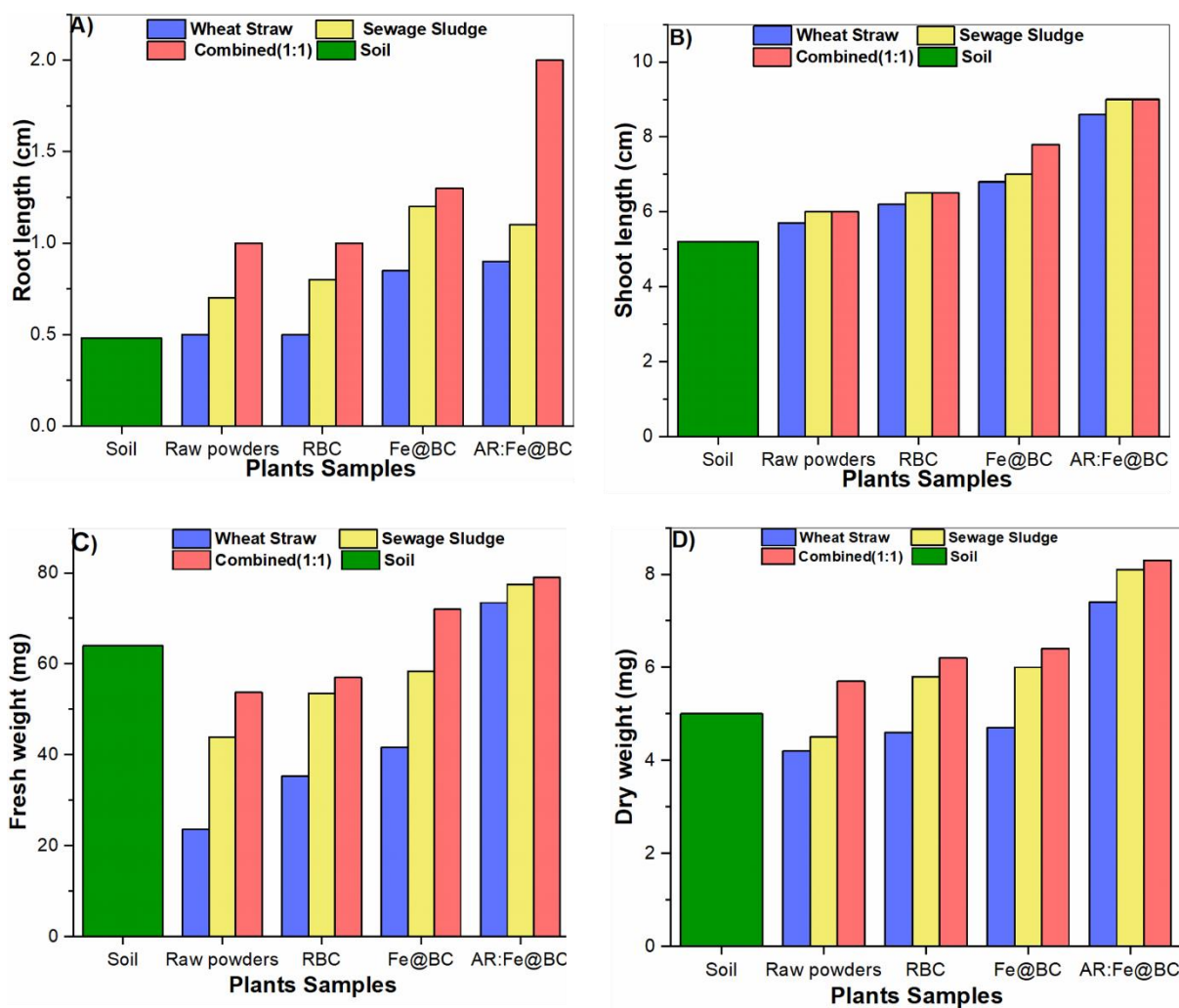
Figure 9 **(A)** Root length, **(B)** Shoot length, **(C)** Fresh weight and, **(D)** Dry weight of mustard plants in pure soil, raw powders, RBC, Fe@BC and AR:Fe@BC

4.10 Practical applications

Current research may contribute to the broader goals of environmental protection, resource conservation, and sustainable development. For instance, the study aims to remove and recover PO_4^{3-} from freshwater reservoirs using Fe@CBC, thus addressing eutrophication concerns in freshwater reservoirs, reducing PO_4^{3-} mining, and mitigating environmental impacts associated with its extraction. The study also employs a sustainable approach by converting waste materials (wheat straw and sewage sludge) into valuable biochar through co-pyrolysis, thus reducing dependence on landfilling or incineration for waste management. Also, utilization of phosphate-sorbed Fe@CBC for mustard plant growth indicates its potential as sustainable alternative to conventional, non-renewable phosphatic fertilizers.

<div align="right">

Chapter 5

</div>

CONCLUSION AND RECOMMENDATIONS

5.1 Conclusion

The feasibility of Fe@CBC as a versatile sorbent for PO_4^{3-} removal from water and subsequent utilization as a phosphatic fertilizer for mustard plant growth was thoroughly investigated. Key findings include Fe@CBC demonstrated exceptional PO_4^{3-} sorption capabilities attributed to its nano porous structure enriched with Fe complexes. Kinetic models (PFO and PSO) provided a satisfactory explanation for the sorption and recovery processes, with PSO yielding a better fit. Freundlich isotherm was found to govern the sorption phenomenon. The dominant mechanisms observed were physisorption and complexation reactions, involving ligand exchange, chemisorption, and electrostatic surface complexation. The incorporation of PO_4^{3-} sorbed Fe@CBC significantly enhanced the growth of mustard plants, highlighting its potential as a sustainable phosphatic fertilizer with promising agricultural benefits.

5.2 Recommendations

Future research should focus on optimizing the preparation of Fe@CBC, evaluating its performance under different conditions, and assessing its long-term stability. Mechanistic insights into the interactions between Fe@CBC and PO_4^{3-} can provide a deeper understanding of the sorption mechanisms involved. Furthermore, it will be crucial to evaluate the economic feasibility and environmental impact of Fe@CBC, as well as its applicability in real-world scenarios and large-scale applications. Exploring the potential of Fe@CBC in removing other contaminants and its multifunctional applications can further enhance its utility.

REFERENCES

Ahmed, A., Abu Bakar, M. S., Sukri, R. S., Hussain, M., Farooq, A., Moogi, S., & Park, Y. K. (2020). Sawdust pyrolysis from the furniture industry in an auger pyrolysis reactor system for biochar and bio-oil production. *Energy Conversion and Management*, *226*. https://doi.org/10.1016/j.enconman.2020.113502

Ajmal, Z., Muhmood, A., Dong, R., & Wu, S. (2020). Probing the efficiency of magnetically modified biomass-derived biochar for effective phosphate removal. *Journal of Environmental Management*, *253*. https://doi.org/10.1016/j.jenvman.2019.109730

Alghamdi, A. A., Al-Odayni, A. B., Saeed, W. S., Al-Kahtani, A., Alharthi, F. A., & Aouak, T. (2019). Efficient adsorption of lead (II) from aqueous phase solutions using polypyrrole-based activated carbon. *Materials*, *12*(12). https://doi.org/10.3390/ma12122020

Almasri, D. A., Saleh, N. B., Atieh, M. A., McKay, G., & Ahzi, S. (2019). Adsorption of phosphate on iron oxide doped halloysite nanotubes. *Scientific Reports*, *9*(1). https://doi.org/10.1038/s41598-019-39035-2

Beaudry, J. W., & Sengupta, S. (2021). Phosphorus recovery from wastewater using pyridine-based ion-exchange resins: Role of impregnated iron oxide nanoparticles and preloaded Lewis acid (Cu2+). *Water Environment Research*, *93*(5), 774–786. https://doi.org/10.1002/wer.1469

Bheel, N., Ibrahim, M. H. W., Adesina, A., Kennedy, C., & Shar, I. A. (2021). Mechanical performance of concrete incorporating wheat straw ash as partial replacement of cement. *Journal of Building Pathology and Rehabilitation*, *6*(1). https://doi.org/10.1007/s41024-020-00099-7

Cao, Y., Shen, G., Zhang, Y., Gao, C., Li, Y., Zhang, P., Xiao, W., & Han, L. (2019). Impacts of carbonization temperature on the Pb(II) adsorption by wheat straw-derived biochar and related mechanism. *Science of the Total Environment*, *692*, 479–489. https://doi.org/10.1016/j.scitotenv.2019.07.102

Dai, Q., Liu, Q., Zhang, X., Cao, L., Hu, B., Shao, J., Ding, F., Guo, X., & Gao, B. (2022). Synergetic effect of co-pyrolysis of sewage sludge and lignin on biochar production and adsorption of methylene blue. *Fuel*, *324*. https://doi.org/10.1016/j.fuel.2022.124587

Das, J., Patra, B. S., Baliarsingh, N., & Parida, K. M. (2006). Adsorption of phosphate by layered double hydroxides in aqueous solutions. *Applied Clay Science*, *32*(3–4), 252–260. https://doi.org/10.1016/j.clay.2006.02.005

Del Nero, M., Galindo, C., Barillon, R., Halter, E., & Madé, B. (2010). Surface reactivity of α-Al2O3 and mechanisms of phosphate sorption: In situ ATR-FTIR spectroscopy and ζ potential studies. *Journal of Colloid and Interface Science*, *342*(2), 437–444. https://doi.org/10.1016/j.jcis.2009.10.057

Deng, Y., Li, M., Zhang, Z., Liu, Q., Jiang, K., Tian, J., Zhang, Y., & Ni, F. (2021). Comparative study on characteristics and mechanism of phosphate adsorption on Mg/Al modified biochar. *Journal of Environmental Chemical Engineering*, *9*(2). https://doi.org/10.1016/j.jece.2021.105079

Dutta, T., Kwon, E., Bhattacharya, S. S., Jeon, B. H., Deep, A., Uchimiya, M., & Kim, K. H. (2017). Polycyclic aromatic hydrocarbons and volatile organic compounds in biochar and biochar-amended soil: a review. In *GCB Bioenergy* (Vol. 9, Issue 6, pp. 990–1004). Blackwell Publishing Ltd. https://doi.org/10.1111/gcbb.12363

Ediene, V., & Umoetok, S. (2017). Concentration of Heavy Metals in Soils at the Municipal Dumpsite in Calabar Metropolis. *Asian Journal of Environment & Ecology*, *3*(2), 1–11. https://doi.org/10.9734/ajee/2017/34236

Estefan, G., Sommer, R., & Ryan, J. (2013). *Methods of Soil, Plant, and Water Analysis: A manual for the West Asia and North Africa region*. www.icarda.org

Feng, Y., Luo, Y., He, Q., Zhao, D., Zhang, K., Shen, S., & Wang, F. (2021). Performance and mechanism of a biochar-based Ca-La composite for the adsorption of phosphate from water. *Journal of Environmental Chemical Engineering*, *9*(3). https://doi.org/10.1016/j.jece.2021.105267

Geelhoed, J. S., Hiemstra, T., & Van Riemsdijk, W. H. (1997). Phosphate and sulfate adsorption on goethite: Single anion and competitive adsorption. In *Geochimica et Cosmochimica Acta* (Vol. 61, Issue 12).

Gilbert, N. (2009). 716–718. In *Environment: the disappearing nutrient* (Vol. 461, pp. 716–718).

Günay, A., Arslankaya, E., & Tosun, I. (2007a). Lead removal from aqueous solution by natural and pretreated clinoptilolite: Adsorption equilibrium and kinetics. *Journal of Hazardous Materials*, *146*(1–2), 362–371. https://doi.org/10.1016/j.jhazmat.2006.12.034

Günay, A., Arslankaya, E., & Tosun, I. (2007b). Lead removal from aqueous solution by natural and pretreated clinoptilolite: Adsorption equilibrium and kinetics. *Journal of Hazardous Materials*, *146*(1–2), 362–371. https://doi.org/10.1016/j.jhazmat.2006.12.034

He, J., Xu, Y., Shao, P., Yang, L., Sun, Y., Yang, Y., Cui, F., & Wang, W. (2020). Modulation of coordinative unsaturation degree and valence state for cerium-based adsorbent to boost phosphate adsorption. *Chemical Engineering Journal*, *394*. https://doi.org/10.1016/j.cej.2020.124912

He, R., Yuan, X., Huang, Z., Wang, H., Jiang, L., Huang, J., Tan, M., & Li, H. (2019). Activated biochar with iron-loading and its application in removing Cr (VI) from aqueous solution. *Colloids and Surfaces A: Physicochemical and Engineering Aspects*, *579*. https://doi.org/10.1016/j.colsurfa.2019.123642

Huang, Y., Lee, X., Grattieri, M., Yuan, M., Cai, R., Macazo, F. C., & Minteer, S. D. (2020a). Modified biochar for phosphate adsorption in environmentally relevant conditions. *Chemical Engineering Journal*, *380*. https://doi.org/10.1016/j.cej.2019.122375

Huang, Y., Lee, X., Grattieri, M., Yuan, M., Cai, R., Macazo, F. C., & Minteer, S. D. (2020b). Modified biochar for phosphate adsorption in environmentally relevant conditions. *Chemical Engineering Journal*, *380*. https://doi.org/10.1016/j.cej.2019.122375

Inam, M. A., Khan, R., Inam, M. W., & Yeom, I. T. (2021). Kinetic and isothermal sorption of antimony oxyanions onto iron hydroxide during water treatment by coagulation process. *Journal of Water Process Engineering*, *41*. https://doi.org/10.1016/j.jwpe.2021.102050

Inam, M. A., Khan, R., Park, D. R., Ali, B. A., Uddin, A., & Yeom, I. T. (2018). Influence of pH and contaminant redox form on the competitive removal of arsenic and antimony from aqueous media by coagulation. *Minerals*, *8*(12). https://doi.org/10.3390/min8120574

Inam, M. A., Khan, R., Park, D. R., Khan, S., Uddin, A., & Yeom, I. T. (2019). Complexation of antimony with natural organic matter: Performance evaluation during coagulation-flocculation process. *International Journal of Environmental Research and Public Health*, *16*(7). https://doi.org/10.3390/ijerph16071092

Jabborova, D., Annapurna, K., Paul, S., Kumar, S., Saad, H. A., Desouky, S., Ibrahim, M. F. M., & Elkelish, A. (2021). Beneficial features of biochar and arbuscular mycorrhiza for improving spinach plant growth, root morphological traits, physiological properties, and soil enzymatic activities. *Journal of Fungi*, *7*(7). https://doi.org/10.3390/jof7070571

Jiang, X., Li, S., Xiang, G., Li, Q., Fan, L., He, L., & Gu, K. (2016). Determination of the acid values of edible oils via FTIR spectroscopy based on the O-H stretching band. *Food Chemistry*, *212*, 585–589. https://doi.org/10.1016/j.foodchem.2016.06.035

Jing, F., Chen, C., Chen, X., Liu, W., Wen, X., Hu, S., Yang, Z., Guo, B., Xu, Y., & Yu, Q. (2020). Effects of wheat straw derived biochar on cadmium availability in a paddy soil and its accumulation in rice. *Environmental Pollution*, *257*. https://doi.org/10.1016/j.envpol.2019.113592

Khayyun, T. S., & Mseer, A. H. (2019). Comparison of the experimental results with the Langmuir and Freundlich models for copper removal on limestone adsorbent. *Applied Water Science*, *9*(8). https://doi.org/10.1007/s13201-019-1061-2

Lee, Y. E., Jeong, Y., Shin, D. C., Yoo, Y. S., Ahn, K. H., Jung, J., & Kim, I. T. (2022). Effects of demineralization on food waste biochar for co-firing: Behaviors of alkali and alkaline earth metals and chlorine. *Waste Management*, *137*, 190–199. https://doi.org/10.1016/j.wasman.2021.10.040

Leo, C. P., Chai, W. K., Mohammad, A. W., Qi, Y., Hoedley, A. F. A., & Chai, S. P. (2011). Phosphorus removal using nanofiltration membranes. *Water Science and Technology*, *64*(1), 199–205. https://doi.org/10.2166/wst.2011.598

Li, D., Shan, R., Jiang, L., Gu, J., Zhang, Y., Yuan, H., & Chen, Y. (2022). A review on the migration and transformation of heavy metals in the process of sludge pyrolysis. In *Resources, Conservation and Recycling* (Vol. 185). Elsevier B.V. https://doi.org/10.1016/j.resconrec.2022.106452

Li, J., Cao, L., Li, B., Huang, H., Yu, W., Sun, C., Long, K., & Young, B. (2023a). Utilization of activated sludge and shell wastes for the preparation of Ca-loaded biochar for phosphate removal and recovery. *Journal of Cleaner Production*, *382*. https://doi.org/10.1016/j.jclepro.2022.135395

Li, J., Cao, L., Li, B., Huang, H., Yu, W., Sun, C., Long, K., & Young, B. (2023b). Utilization of activated sludge and shell wastes for the preparation of Ca-loaded biochar for

phosphate removal and recovery. *Journal of Cleaner Production*, *382*. https://doi.org/10.1016/j.jclepro.2022.135395

Li, J., Li, B., Huang, H., Lv, X., Zhao, N., Guo, G., & Zhang, D. (2019a). Removal of phosphate from aqueous solution by dolomite-modified biochar derived from urban dewatered sewage sludge. *Science of the Total Environment*, *687*, 460–469. https://doi.org/10.1016/j.scitotenv.2019.05.400

Li, J., Li, B., Huang, H., Lv, X., Zhao, N., Guo, G., & Zhang, D. (2019b). Removal of phosphate from aqueous solution by dolomite-modified biochar derived from urban dewatered sewage sludge. *Science of the Total Environment*, *687*, 460–469. https://doi.org/10.1016/j.scitotenv.2019.05.400

Liu, B., Gai, S., Lan, Y., Cheng, K., & Yang, F. (2022). Metal-based adsorbents for water eutrophication remediation: A review of performances and mechanisms. In *Environmental Research* (Vol. 212). Academic Press Inc. https://doi.org/10.1016/j.envres.2022.113353

Liu, D., Qian, K., He, Y. B., Luo, D., Li, H., Wu, M., Kang, F., & Li, B. (2018). Positive film-forming effect of fluoroethylene carbonate (FEC) on high-voltage cycling with three-electrode LiCoO2/Graphite pouch cell. *Electrochimica Acta*, *269*, 378–387. https://doi.org/10.1016/j.electacta.2018.02.151

Liu, M., Li, R., Wang, J., Liu, X., Li, S., & Shen, W. (2022). Recovery of phosphate from aqueous solution by dewatered dry sludge biochar and its feasibility in fertilizer use. *Science of the Total Environment*, *814*. https://doi.org/10.1016/j.scitotenv.2021.152752

Liu, X. Q., Ding, H. S., Wang, Y. Y., Liu, W. J., & Jiang, H. (2016). Pyrolytic Temperature Dependent and Ash Catalyzed Formation of Sludge Char with Ultra-High Adsorption to 1-Naphthol. *Environmental Science and Technology*, *50*(5), 2602–2609. https://doi.org/10.1021/acs.est.5b04536

Liu, Z., & Balasubramanian, R. (2013). A comparison of thermal behaviors of raw biomass, pyrolytic biochar and their blends with lignite. *Bioresource Technology*, *146*, 371–378. https://doi.org/10.1016/j.biortech.2013.07.072

Maugé, F., Lamotte, J., Nesterenko, N. S., Manoilova, O., & Tsyganenko, A. A. (2001). FT-IR study of surface properties of unsupported MoS 2. In *Catalysis Today* (Vol. 70).

Mengel, K. , K. E. A. , K. H. , & A. T. (2001). Phosphorus. In *Principles of Plant Nutrition* (pp. 453–479).

Mukherjee, A., Zimmerman, A. R., & Harris, W. (2011). Surface chemistry variations among a series of laboratory-produced biochars. *Geoderma*, *163*(3–4), 247–255. https://doi.org/10.1016/j.geoderma.2011.04.021

Nguyen, T. H., Pham, T. H., Nguyen Thi, H. T., Nguyen, T. N., Nguyen, M. V., Tran Dinh, T., Nguyen, M. P., Do, T. Q., Phuong, T., Hoang, T. T., Mai Hung, T. T., & Thi, V. H. T. (2019). Synthesis of Iron-Modified Biochar Derived from Rice Straw and Its Application to Arsenic Removal. *Journal of Chemistry*, *2019*. https://doi.org/10.1155/2019/5295610

Niazi, N. K., Bibi, I., Shahid, M., Ok, Y. S., Shaheen, S. M., Rinklebe, J., Wang, H., Murtaza, B., Islam, E., Farrakh Nawaz, M., & Lüttge, A. (2018). Arsenic removal by Japanese oak wood biochar in aqueous solutions and well water: Investigating arsenic fate using integrated spectroscopic and microscopic techniques. *Science of the Total Environment*, *621*, 1642–1651. https://doi.org/10.1016/j.scitotenv.2017.10.063

Owens, L. B., & Shipitalo, M. J. (2006). Surface and Subsurface Phosphorus Losses from Fertilized Pasture Systems in Ohio. *Journal of Environmental Quality*, *35*(4), 1101–1109. https://doi.org/10.2134/jeq2005.0402

Owodunni, A. A., Ismail, S., Kurniawan, S. B., Ahmad, A., Imron, M. F., & Abdullah, S. R. S. (2023). A review on revolutionary technique for phosphate removal in wastewater using green coagulant. In *Journal of Water Process Engineering* (Vol. 52). Elsevier Ltd. https://doi.org/10.1016/j.jwpe.2023.103573

Ren, L., Li, Y., Wang, K., Ding, K., Sha, M., Cao, Y., Kong, F., & Wang, S. (2021). Recovery of phosphorus from eutrophic water using nano zero-valent iron-modified biochar and its utilization. *Chemosphere*, *284*. https://doi.org/10.1016/j.chemosphere.2021.131391

Ren, Y., Zheng, W., Duan, X., Goswami, N., & Liu, Y. (2022). Recent advances in electrochemical removal and recovery of phosphorus from water: A review. *Environmental Functional Materials*, *1*(1), 10–20. https://doi.org/10.1016/j.efmat.2022.04.003

Riaz, U., Murtaza, G., Saifullah, Farooq, M., Aziz, H., Qadir, A. A., Mehdi, S. M., & Qazi, M. A. (2020). Chemical fractionation and risk assessment of trace elements in sewage

sludge generated from various states of Pakistan. *Environmental Science and Pollution Research*, *27*(32), 39742–39752. https://doi.org/10.1007/s11356-020-07795-4

Sabadash, V., Gumnitsky, J., & Hyvlyud, A. (2016). Mechanism of Phosphates Sorption by Zeolites Depending on Degree of their Substitution MECHANISM OF PHOSPHATES SORPTION BY ZEOLITES DEPENDING ON DEGREE OF THEIR SUBSTITUTION FOR POTASSIUM IONS. In *CHEMISTRY & CHEMICAL TECHNOLOGY* (Vol. 10, Issue 2).

Sahu, S., Bishoyi, N., Sahu, M. K., & Patel, R. K. (2021). Investigating the selectivity and interference behavior for detoxification of Cr(VI) using lanthanum phosphate polyaniline nanocomposite via adsorption-reduction mechanism. *Chemosphere*, *278*. https://doi.org/10.1016/j.chemosphere.2021.130507

Sakhiya, A. K., Anand, A., & Kaushal, P. (2020). Production, activation, and applications of biochar in recent times. In *Biochar* (Vol. 2, Issue 3, pp. 253–285). Springer Science and Business Media B.V. https://doi.org/10.1007/s42773-020-00047-1

Salim, N. A. A., Fulazzaky, M. A., Puteh, M. H., Khamidun, M. H., Yusoff, A. R. M., Abdullah, N. H., Ahmad, N., Lazim, Z. M., & Nuid, M. (2021). Adsorption of phosphate from aqueous solution onto iron-coated waste mussel shell: Physicochemical characteristics, kinetic, and isotherm studies. *Biointerface Research in Applied Chemistry*, *11*(5), 12831–12842. https://doi.org/10.33263/BRIAC115.1283112842

Shackley, S., Hammond, J., Gaunt, J., & Ibarrola, R. (2011). The feasibility and costs of biochar deployment in the UK. In *Carbon Management* (Vol. 2, Issue 3, pp. 335–356). https://doi.org/10.4155/cmt.11.22

Shakoor, M. B., Ye, Z. L., & Chen, S. (2021). Engineered biochars for recovering phosphate and ammonium from wastewater: A review. In *Science of the Total Environment* (Vol. 779). Elsevier B.V. https://doi.org/10.1016/j.scitotenv.2021.146240

Shan, S., Tang, H., Zhao, Y., Wang, W., & Cui, F. (2019). Highly porous zirconium-crosslinked graphene oxide/alginate aerogel beads for enhanced phosphate removal. *Chemical Engineering Journal*, *359*, 779–789. https://doi.org/10.1016/j.cej.2018.10.033

Singh, S., Kumar, V., Dhanjal, D. S., Datta, S., Bhatia, D., Dhiman, J., Samuel, J., Prasad, R., & Singh, J. (2020). A sustainable paradigm of sewage sludge biochar: Valorization,

opportunities, challenges and future prospects. In *Journal of Cleaner Production* (Vol. 269). Elsevier Ltd. https://doi.org/10.1016/j.jclepro.2020.122259

Suazo-Hernández, J., Sepúlveda, P., Cáceres-Jensen, L., Castro-Rojas, J., Poblete-Grant, P., Bolan, N., & Mora, M. de la L. (2023). nZVI-Based Nanomaterials Used for Phosphate Removal from Aquatic Systems. In *Nanomaterials* (Vol. 13, Issue 3). MDPI. https://doi.org/10.3390/nano13030399

Sun, Y., Zhao, Q., Luo, C., Wang, G., Sun, Y., & Yan, K. (2019). A Novel Strategy for the Synthesis of Fe3(PO4)2 Using Fe-P Waste Slag and CO2 Followed by Its Use as the Precursor for LiFePO4 Preparation. *ACS Omega*, *4*(6), 9932–9938. https://doi.org/10.1021/acsomega.9b01074

Tang, Q., Shi, C., Shi, W., Huang, X., Ye, Y., Jiang, W., Kang, J., Liu, D., Ren, Y., & Li, D. (2019). Preferable phosphate removal by nano-La(III) hydroxides modified mesoporous rice husk biochars: Role of the host pore structure and point of zero charge. *Science of the Total Environment*, *662*, 511–520. https://doi.org/10.1016/j.scitotenv.2019.01.159

Venkatesh, G., Gopinath, K. A., Reddy, K. S., Reddy, B. S., Prabhakar, M., Srinivasarao, C., Kumari, V. V., & Singh, V. K. (2022). Characterization of Biochar Derived from Crop Residues for Soil Amendment, Carbon Sequestration and Energy Use. *Sustainability (Switzerland)*, *14*(4). https://doi.org/10.3390/su14042295

Wang, S., Gao, B., Li, Y., Wan, Y., & Creamer, A. E. (2015). Sorption of arsenate onto magnetic iron-manganese (Fe-Mn) biochar composites. *RSC Advances*, *5*(83), 67971–67978. https://doi.org/10.1039/c5ra12137j

Wang, Y., Weng, W., Xu, H., Luo, Y., Guo, D., Li, D., & Li, D. (2019). Negatively charged molybdate mediated nitrogen-doped graphene quantum dots as a fluorescence turn on probe for phosphate ion in aqueous media and living cells. *Analytica Chimica Acta*, *1080*, 196–205. https://doi.org/10.1016/j.aca.2019.07.023

WHO. (2017). *Guidelines for Drinking-water Quality*.

Xiong, Q., Wu, X., Lv, H., Liu, S., Hou, H., & Wu, X. (2021). Influence of rice husk addition on phosphorus fractions and heavy metals risk of biochar derived from sewage sludge. *Chemosphere*, *280*. https://doi.org/10.1016/j.chemosphere.2021.130566

Yang, Q., Wang, X., Luo, W., Sun, J., Xu, Q., Chen, F., Zhao, J., Wang, S., Yao, F., Wang, D., Li, X., & Zeng, G. (2018a). Effectiveness and mechanisms of phosphate adsorption on

iron-modified biochars derived from waste activated sludge. *Bioresource Technology*, *247*, 537–544. https://doi.org/10.1016/j.biortech.2017.09.136

Yang, Q., Wang, X., Luo, W., Sun, J., Xu, Q., Chen, F., Zhao, J., Wang, S., Yao, F., Wang, D., Li, X., & Zeng, G. (2018b). Effectiveness and mechanisms of phosphate adsorption on iron-modified biochars derived from waste activated sludge. *Bioresource Technology*, *247*, 537–544. https://doi.org/10.1016/j.biortech.2017.09.136

Yang, Y., Zhao, Y. Q., Babatunde, A. O., Wang, L., Ren, Y. X., & Han, Y. (2006). Characteristics and mechanisms of phosphate adsorption on dewatered alum sludge. *Separation and Purification Technology*, *51*(2), 193–200. https://doi.org/10.1016/j.seppur.2006.01.013

Zeng, S., & Kan, E. (2022). FeCl3-activated biochar catalyst for heterogeneous Fenton oxidation of antibiotic sulfamethoxazole in water. *Chemosphere*, *306*. https://doi.org/10.1016/j.chemosphere.2022.135554

Zhu, B., Fan, T., & Zhang, D. (2008). Adsorption of copper ions from aqueous solution by citric acid modified soybean straw. *Journal of Hazardous Materials*, *153*(1–2), 300–308. https://doi.org/10.1016/j.jhazmat.2007.08.050

MS Thesis

PRIMARY SOURCES

1	link.springer.com Internet Source	1%
2	Muhammad Ali Inam, Rizwan Khan, Muhammad Waleed Inam, Ick Tae Yeom. "Kinetic and isothermal sorption of antimony oxyanions onto iron hydroxide during water treatment by coagulation process", Journal of Water Process Engineering, 2021 Publication	1%
3	www.mdpi.com Internet Source	1%
4	Submitted to Higher Education Commission Pakistan Student Paper	1%
5	Jing Li, Lu Cao, Bing Li, Haiming Huang, Wei Yu, Cairui Sun, Kehua Long, Brent Young. "Utilization of activated sludge and shell wastes for the preparation of Ca-loaded biochar for phosphate removal and recovery", Journal of Cleaner Production, 2022	1%

Publication

6 Jayalakshmi R., Jeyanthi J.. "Simultaneous removal of binary dye from textile effluent using cobalt ferrite-alginate nanocomposite: Performance and mechanism", Microchemical Journal, 2019
Publication
<1 %

7 Submitted to University of Greenwich
Student Paper
<1 %

8 Waleed Usmani, Muhammad Ali Inam, Rashid Iftikhar, Iqra Irfan et al. "Efficient removal of hexavalent chromium Cr (VI) using magnesium-iron layered double hydroxide supported on orange peel (Mg-Fe LDH@OPP): A synthetic experimental and mechanism studies", Journal of Water Process Engineering, 2023
Publication
<1 %

9 www.slideshare.net
Internet Source
<1 %

10 Peijing Kuang, Yubo Cui, Zhongwei Zhang, Kedong Ma, Wanjun Zhang, Ke Zhao, Xiaomeng Zhang. "Increasing Surface Functionalities of FeCl3-Modified Reed Waste Biochar for Enhanced Nitrate Adsorption Property", Processes, 2023
Publication
<1 %

11 assets.researchsquare.com
Internet Source
<1%

12 Submitted to University of Edinburgh
Student Paper
<1%

13 Submitted to Taylor's Education Group
Student Paper
<1%

14 erepository.uonbi.ac.ke
Internet Source
<1%

15 utpedia.utp.edu.my
Internet Source
<1%

16 downloads.hindawi.com
Internet Source
<1%

17 Li Wang, Jingyi Wang, Zixuan Wang, Chi He, Wei Lyu, Wei Yan, Liu Yang. "Enhanced antimonate (Sb(V)) removal from aqueous solution by La-doped magnetic biochars", Chemical Engineering Journal, 2018
Publication
<1%

18 tesisenred.net
Internet Source
<1%

19 Sana Zainab, Sajal Fraz, Saif Ullah Awan, Danish Hussain, Syed Rizwan, Waqar Mehmood. "Optimized time dependent exfoliation of graphite for fabrication of Graphene/GO/GrO nanocomposite based
<1%

pseudo-supercapacitor", Scientific Reports, 2023
Publication

20   m.scirp.org
     Internet Source   <1%

21   www.hindawi.com
     Internet Source   <1%

22   Jing Li, Bing Li, Haiming Huang, Xiaomei Lv,   <1%
     Ning Zhao, Guojun Guo, Dingding Zhang.
     "Removal of phosphate from aqueous
     solution by dolomite-modified biochar derived
     from urban dewatered sewage sludge",
     Science of The Total Environment, 2019
     Publication

23   Submitted to University of Leeds
     Student Paper   <1%

24   d-nb.info
     Internet Source   <1%

25   dspace.knust.edu.gh
     Internet Source   <1%

26   scholarship.rice.edu
     Internet Source   <1%

27   www.nature.com
     Internet Source   <1%

28   Submitted to Universiti Teknologi MARA
     Student Paper   <1%

29 Submitted to University of Glasgow
Student Paper
<1 %

30 coek.info
Internet Source
<1 %

31 theses.ncl.ac.uk
Internet Source
<1 %

32 www.springerplus.com
Internet Source
<1 %

33 Xiaomin Liu, Bin Li, Yufeng Wu. "The pretreatment of non-ferrous metallurgical waste slag and its research progress in the preparation of glass-ceramics", Journal of Cleaner Production, 2023
Publication
<1 %

34 rosdok.uni-rostock.de
Internet Source
<1 %

35 Submitted to Georgia Institute of Technology Main Campus
Student Paper
<1 %

36 Submitted to VIT University
Student Paper
<1 %

37 dns2.asia.edu.tw
Internet Source
<1 %

38 Hua Zhang, Zhenyu Wu, Qingliang Shi, Awais Khan et al. "Fabrication and characterization
<1 %

of magnetic eucalyptus carbon for efficient Cr(VI) removal in aqueous solution and its mechanisms", Arabian Journal of Chemistry, 2023
Publication

39   Elisee Nsimba Bakatula, Dominique Richard, Carmen Mihaela Neculita, Gerald J. Zagury. "Determination of point of zero charge of natural organic materials", Environmental Science and Pollution Research, 2018
Publication

<1%

40   Eric F. Zama, Yong-Guan Zhu, Brian J. Reid, Gou-Xin Sun. "The role of biochar properties in influencing the sorption and desorption of Pb(II), Cd(II) and As(III) in aqueous solution", Journal of Cleaner Production, 2017
Publication

<1%

41   Ming, Z.W.. "Synergistic adsorption of phenol from aqueous solution onto polymeric adsorbents", Journal of Hazardous Materials, 20060206
Publication

<1%

42   Y. Gong, D. Zhao. "Physical–Chemical Processes for Phosphorus Removal and Recovery", Elsevier BV, 2014
Publication

<1%

43   bioresources.cnr.ncsu.edu
Internet Source

<1%

44 Submitted to Addis Ababa University
Student Paper
<1%

45 Submitted to Coventry University
Student Paper
<1%

46 Endar Hidayat, Nur Maisarah Binti Mohamad Sarbani, Seiichiro Yonemura, Yoshiharu Mitoma, Hiroyuki Harada. "Application of Box–Behnken Design to Optimize Phosphate Adsorption Conditions from Water onto Novel Adsorbent CS-ZL/ZrO/Fe3O4: Characterization, Equilibrium, Isotherm, Kinetic, and Desorption Studies", International Journal of Molecular Sciences, 2023
Publication
<1%

47 Junhui Zhang, Jiacong Chen, Jingyong Liu, Fatih Evrendilek, Gang Zhang, Zhibin Chen, Shengzheng Huang, Shuiyu Sun. "Fates of heavy metals, S, and P during co-combustion of textile dyeing sludge and cattle manure", Journal of Cleaner Production, 2022
Publication
<1%

48 Submitted to Universiti Sains Malaysia
Student Paper
<1%

49 Submitted to University of Nottingham
Student Paper
<1%

50 apessay.elementfx.com
Internet Source
<1%

| 51 | nadre.ethernet.edu.et
Internet Source | <1% |

| 52 | repository.sustech.edu
Internet Source | <1% |

| 53 | repository.up.ac.za
Internet Source | <1% |

| 54 | www.tandfonline.com
Internet Source | <1% |

| 55 | Hasnain Isa, M.. "Low cost removal of disperse dyes from aqueous solution using palm ash", Dyes and Pigments, 2007
Publication | <1% |

| 56 | Submitted to Midlands State University
Student Paper | <1% |

| 57 | Submitted to UNESCO-IHE Institute for Water Education
Student Paper | <1% |

| 58 | eprints.nottingham.ac.uk
Internet Source | <1% |

| 59 | iwaponline.com
Internet Source | <1% |

| 60 | Qingliang Cui, Jinling Xu, Wei Wang, Lianshuai Tan, Yongxing Cui, Tongtong Wang, Gaoliang Li, Diao She, Jiyong Zheng. "Phosphorus recovery by core-shell γ-Al2O3/Fe3O4 biochar | <1% |

composite from aqueous phosphate solutions", Science of The Total Environment, 2020
Publication

61 Submitted to University of South Australia
Student Paper
<1%

62 pubmed.ncbi.nlm.nih.gov
Internet Source
<1%

63 De-Chang Li, Wan-Fei Xu, Yang Mu, Han-Qing Yu, Hong Jiang, John C. Crittenden. "Remediation of Petroleum-Contaminated Soil and Simultaneous Recovery of Oil by Fast Pyrolysis", Environmental Science & Technology, 2018
Publication
<1%

64 Jie Yang, Mingliang Zhang, Haixia Wang, Junbing Xue, Qi Lv, Guibin Pang. "Efficient Recovery of Phosphate from Aqueous Solution Using Biochar Derived from Co-pyrolysis of Sewage Sludge with Eggshell", Journal of Environmental Chemical Engineering, 2021
Publication
<1%

65 Li, Tingqiang, Xuan Han, Chengfeng Liang, M.J.I. Shohag, and Xiaoe Yang. "Sorption of sulphamethoxazole by the biochars derived from rice straw and alligator flag", Environmental Technology, 2015.

66 Lu Cao, Zhu Ouyang, Tao Chen, Haiming Huang, Mingge Zhang, Ziyang Tai, Kehua Long, Cairui Sun, Bingqian Wang. "Phosphate removal from aqueous solution using calcium-rich biochar prepared by the pyrolysis of crab shells", Environmental Science and Pollution Research, 2022

Publication

<1%

67 Yu Deng, Min Li, Zhan Zhang, Qiao Liu, Kele Jiang, Jingjie Tian, Ying Zhang, Fuquan Ni. "Comparative Study on Characteristics and Mechanism of Phosphate Adsorption on Mg/Al Modified Biochar", Journal of Environmental Chemical Engineering, 2021

Publication

<1%

68 static.frontiersin.org
Internet Source

<1%

69 Isha Medha, Subhash Chandra, Vanapalli Kumar Raja, Biswajit Samal, Jayanta Bhattacharya, Bidus Kanti Das. "(3-Aminopropyl)triethoxysilane and iron rice straw biochar composites for the sorption of Cr (VI) and Zn (II) using the extract of heavy metals contaminated soil", Science of The Total Environment, 2021

Publication

<1%

70   J. Kholová. "Response of maize genotypes to salinity stress in relation to osmolytes and metal-ions contents, oxidative stress and antioxidant enzymes activity", Biologia Plantarum, 06/2009

Publication

<1 %

71   Jing Lu, Yaqian Yang, Pengxiao Liu, Ying Li, Fei Huang, Liqin Zeng, Yuze Liang, Siyuan Li, Bin Hou. "Iron-montmorillonite treated corn straw biochar: Interfacial chemical behavior and stability", Science of The Total Environment, 2020

Publication

<1 %

72   Junjie Su, Han Hao, Xiaofan Lv, Xin Jin, Qi Yang. "Properties and mechanism of hexavalent chromium removal by FeS@ graphite carbon nitride nanocomposites", Colloids and Surfaces A: Physicochemical and Engineering Aspects, 2020

Publication

<1 %

73   McGuire, Molly M., and Ellen K. Herman. "A novel ATR-FTIR technique for identifying colloid composition in natural waters : ATR-FTIR TECHNIQUE FOR IDENTIFYING COLLOID COMPOSITION", Hydrological Processes, 2014.

Publication

<1 %

74 Muhammad Ali Inam, Kang Hoon Lee, Hira Lal Soni, Kashif Hussain Mangi et al. "Coagulation Behavior of Antimony Oxyanions in Water: Influence of pH, Inorganic and Organic Matter on the Physicochemical Characteristics of Iron Precipitates", Molecules, 2022
Publication

<1 %

75 R. Gamal, S.E. Rizk, N.E. El-Hefny. "The adsorptive removal of Mo(VI) from aqueous solution by a synthetic magnetic chromium ferrite nanocomposite using a nonionic surfactant", Journal of Alloys and Compounds, 2020
Publication

<1 %

76 Sainan Xia, Shengrong Liang, Yixue Qin, Weijie Chen, Bin Xue, Bingbing Zhang, Guomin Xu. "Significant Improvement of Adsorption for Phosphate Removal by Lanthanum-Loaded Biochar", ACS Omega, 2023
Publication

<1 %

77 Wanlu Li, Gege Cai, Kun Luo, Jiejun Zhang, Haibin Li, Guolian Li, Jiamei Zhang, Xing Chen, Fazhi Xie. "Synthesis of magnesium-modified ceramsite from iron tailings as efficient adsorbent for phosphorus removal", Separation and Purification Technology, 2023

<1 %

Publication

78 Zuhao Chen, Huayong Luo, Hongwei Rong. "Development of polyaminated chitosan-zirconium(IV) complex bead adsorbent for highly efficient removal and recovery of phosphorus in aqueous solutions", International Journal of Biological Macromolecules, 2020
Publication
<1%

79 ebin.pub
Internet Source
<1%

80 eprints.utem.edu.my
Internet Source
<1%

81 jhs.mazums.ac.ir
Internet Source
<1%

82 journals.srbiau.ac.ir
Internet Source
<1%

83 psaspb.upm.edu.my
Internet Source
<1%

84 www.iiste.org
Internet Source
<1%

85 www.scielo.br
Internet Source
<1%

86 www.scribd.com
Internet Source
<1%

87　"Biochar Applications in Agriculture and Environment Management", Springer Science and Business Media LLC, 2020
Publication

<1%

88　Ashitha Gopinath, G. Divyapriya, Vartika Srivastava, A.R. Laiju, P.V. Nidheesh, M. Suresh Kumar. "Conversion of sewage sludge into biochar: A potential resource in water and wastewater treatment", Environmental Research, 2021
Publication

<1%

89　Bing Liu, Shuang Gai, Yibo Lan, Kui Cheng, Fan Yang. "Metal-based adsorbents for water eutrophication remediation: A review of performances and mechanisms", Environmental Research, 2022
Publication

<1%

90　Hifsa Khurshid, Muhammad Raza Ul Mustafa, Umer Rashid, Mohamed Hasnain Isa, Yeek Chia Ho, Mumtaz Muhammad Shah. "Adsorptive removal of COD from produced water using tea waste biochar", Environmental Technology & Innovation, 2021
Publication

<1%

91　Isha Medha, Subhash Chandra, Kumar Raja Vanapalli, Biswajit Samal, Jayanta Bhattacharya, Bidus Kanti Das. "(3-Aminopropyl)triethoxysilane and iron rice

<1%

straw biochar composites for the sorption of Cr (VI) and Zn (II) using the extract of heavy metals contaminated soil", Science of The Total Environment, 2021
Publication

92 Jinqi Zhu, Tingwei Rui, Yiwen You, Dong Shen, Tao Liu. "Magnetic biochar with Mg/La modification for highly effective phosphate adsorption and its potential application as an algaecide and fertilizer", Environmental Research, 2023
Publication

<1 %

93 M. Halalsheh, K. Shatanawi, R. Shawabkeh, G.R. Kassab et al. "Impact of temperature and residence time on sewage sludge pyrolysis for combined carbon sequestration and energy production", Heliyon, 2023
Publication

<1 %

94 Ran Xiao, Han Zhang, Zhineng Tu, Ronghua Li, Songling Li, Zhongyang Xu, Zengqiang Zhang. "Enhanced removal of phosphate and ammonium by MgO-biochar composites with NH3·H2O hydrolysis pretreatment", Environmental Science and Pollution Research, 2019
Publication

<1 %

95 Raveen Fatima, Shazia Iram. "A model of eco-friendly cooking stove and a potential

<1 %

application of soot for remediation of heavy metals in the environment", Energy Sources, Part A: Recovery, Utilization, and Environmental Effects, 2020
Publication

96   Shuoxun Dong, Qinghua Ji, Yili Wang, Huijuan Liu, Jiuhui Qu. "Enhanced phosphate removal using zirconium hydroxide encapsulated in quaternized cellulose", Journal of Environmental Sciences, 2020
Publication   <1%

97   Zeyu Fan, Xian Zhou, Ziling Peng, Sha Wan, Zhuo Fan Gao, Shanshan Deng, Luling Tong, Wei Han, Xia Chen. "Co-pyrolysis technology for enhancing the functionality of sewage sludge biochar and immobilizing heavy metals", Chemosphere, 2023
Publication   <1%

98   b3b7dd1a-d8cb-4579-8cfc-f21897e0f1ee.filesusr.com
Internet Source   <1%

99   chemeng.hust.edu.vn
Internet Source   <1%

100 digiresearch.vut.ac.za
Internet Source   <1%

101 dokumen.pub
Internet Source   <1%

102   eprints.lancs.ac.uk
       Internet Source   <1%

103   erepository.uonbi.ac.ke:8080
       Internet Source   <1%

104   espace.curtin.edu.au
       Internet Source   <1%

105   mdpi-res.com
       Internet Source   <1%

106   ouci.dntb.gov.ua
       Internet Source   <1%

107   pure.manchester.ac.uk
       Internet Source   <1%

108   repository.unam.edu.na
       Internet Source   <1%

109   scholarworks.uaeu.ac.ae
       Internet Source   <1%

110   www.repository.unipr.it
       Internet Source   <1%

111   "Arsenic in Plants", Wiley, 2022
       Publication   <1%

112   Carlos E.R. Barquilha, Maria C.B. Braga.   <1%
       "Adsorption of organic and inorganic
       pollutants onto biochars: Challenges,

operating conditions, and mechanisms", Bioresource Technology Reports, 2021
Publication

113 Ronghua Li, Jim J. Wang, Baoyue Zhou, Zengqiang Zhang, Shuai Liu, Shuang Lei, Ran Xiao. "Simultaneous capture removal of phosphate, ammonium and organic substances by MgO impregnated biochar and its potential use in swine wastewater treatment", Journal of Cleaner Production, 2017
Publication
<1 %

114 Danni Li, Rui Shan, Lixia Jiang, Jing Gu, Yuyuan Zhang, Haoran Yuan, Yong Chen. "A review on the migration and transformation of heavy metals in the process of sludge pyrolysis", Resources, Conservation and Recycling, 2022
Publication
<1 %

115 Jianwei Lin, Yuying Zhao, Yanhui Zhan, Yan Wang. "Control of internal phosphorus release from sediments using magnetic lanthanum/iron-modified bentonite as active capping material", Environmental Pollution, 2020
Publication
<1 %

116 S. Rangabhashiyam, Pollyanna V. dos Santos Lins, Leonardo M.T. de Magalhães Oliveira, Pamela Sepulveda et al. "Sewage sludge-
<1 %

derived biochar for the adsorptive removal of wastewater pollutants: A critical review", Environmental Pollution, 2021

Publication

Exclude quotes   Off   Exclude matches   Off
Exclude bibliography   On